8. Tateno C, Yoshizane Y, Saito N, et al. Near completely humanized liver in mice shows human-type metabolic responses to drugs. Am J Pathol **2004**; 165:901–12.
9. Abe A, Inoue K, Tanaka T, et al. Quantitation of hepatitis B virus genomic DNA by real-time detection PCR. J Clin Microbiol **1999**; 37:2899–03.
10. Mason AL, Xu L, Guo L, Kuhns M, Perrillo RP. Molecular basis for persistent hepatitis B virus infection in the liver after clearance of serum hepatitis B surface antigen. Hepatology **1998**; 27:1736–42.
11. Lin HJ, Lai CL, Lau JY, Chung HT, Lauder IJ, Fong MW. Evidence for intrafamilial transmission of hepatitis B virus from sequence analysis of mutant HBV DNAs in two Chinese families. Lancet **1990**; 336:208–12.
12. Thompson JD, Gibson TJ, Plewniak F, et al. The CLUSTAL_X windows interface: flexible strategies for multiple sequence alignment added by quality analysis tools. Nucleic Acids Res **1997**; 25:4876–82.
13. Tamura K, Dudley J, Nei M, Kumar S. MEGA4 Evolutionary Genetics Analysis (MEGA) software version 4.0. Mol Biol Evol **2007**; 24:1596–9.
14. Lin CL, Kao JH, Chen BF, Chen PJ, Lai MY, Chen DS. Application of hepatitis B virus genotyping and phylogenetic analysis in intrafamilial transmission of hepatitis B virus. Clin Infect Dis **2005**; 41:1576–81.
15. Tajiri H, Tanaka Y, Kagimoto S, Murakami J, Tokuhara D, Mizokami M. Molecular evidence of father-to-child transmission of hepatitis B virus. J Med Virol **2007**; 79:922–26.
16. Hoofnagle JH, Seeff LB, Bales ZB, Barker LF. Type B hepatitis after transfusion with blood containing antibody to hepatitis B core antigen. N Engl J Med **1978**; 298:1379–83.
17. Lander JJ, Gitnick GL, Gelb LH, Aach RD. Anticore antibody screening of transfused blood. ox Sang **1978**; 34:77–80.
18. Koziol DE, Holland PV, Alling DW. Antibody to hepatitis B core antigen as a paradoxical marker for non-A, non-B hepatitis agents in donated blood. Ann Intern Med **1986**; 104:488–95.
19. Sugg U, Schenzle D, Hess G. Antibodies to hepatitis B core antigen in blood donors screened for alanine aminotransferase level and hepatitis non-A, non-B in recipients. Transfusion **1988**; 28:386–8.
20. Allain JP. Occult hepatitis B virus infection: implications in transfusion. ox Sang **2004**; 86:83–91.
21. Wands JR, Chura CM, Roll FJ, Maddrey WC. Serial studies of hepatitis-associated antigen and antibody in patients receiving antitumor chemotherapy for myeloproliferative and lymphoproliferative disorders. Gastroenterology **1975**; 68:105–12.
22. Velati C, Romanò L, Fomiatti L, Baruffi L, Zanetti AR; SIMTI Research Group. Impact of nucleic acid testing for hepatitis B virus, hepatitis C virus, and human immunodeficiency virus on the safety of blood supply in Italy: a 6-year survey. Transfusion **2008**; 48:2205–13.
23. Mosley JW, Stevens CE, Aach RD, et al. Donor screening for antibody to hepatitis B core antigen and hepatitis B virus infection in transfusion recipients. Transfusion **1995**; 35:5–12.
24. Satake M, Taira R, Yugi H, et al. Infectivity of blood components with low hepatitis B virus DNA levels identified in a lookback program. Transfusion **2007**; 47:1197–205.
25. Levicnik-Stezinar S, Rahne-Potokar U, Candotti D, Lelie N, Allain JP. Anti-HBs positive occult hepatitis B virus carrier blood infectious in two transfusion recipients. J Hepatol **2008**; 48:1022–5.
26. Yuen MF, Lee CK, Wong DK, et al. Prevalence of occult hepatitis B infection in a highly endemic area for chronic hepatitis B: a study of a large blood donor population. Gut **2010**; 59:1389–93.

EMBO reports

scientific report

Protein phosphatase 1γ is responsible for dephosphorylation of histone H3 at Thr 11 after DNA damage

Midori Shimada[1], Mayumi Haruta[1], Hiroyuki Niida[1], Kazunobu Sawamoto[2] & Makoto Nakanishi[1+]

[1]Department of Cell Biology, and [2]Developmental and Regenerative Biology, Graduate School of Medical Sciences, Nagoya City University, Nagoya, Japan

The DNA-damage-induced transcriptional suppression of cell cycle regulatory genes correlates with a reduction in histone H3-Thr 11 phosphorylation (H3-pThr 11) on their promoters that is partly mediated by the dissociation of Chk1 from chromatin. In this study, we identify protein phosphatase 1γ (PP1γ) as a phosphatase responsible for DNA-damage-induced H3-pThr 11 dephosphorylation. PP1γ is activated after DNA damage, which is mainly mediated by a reduction in Cdk-dependent phosphorylation of PP1γ at Thr 311. The depletion of PP1γ sensitizes HCT116 cells to DNA damage. Our results suggest that the ataxia telangiectasia, mutated and Rad3-related–Chk1 axis regulates H3-pThr 11 dephosphorylation on DNA damage, at least in part by the activation of PP1γ through Chk1-dependent inhibition of Cdks.

Keywords: PP1; DNA damage; transcription; checkpoint; Cdk

EMBO *reports* (2010) 11, 883–889. doi:10.1038/embor.2010.152

INTRODUCTION

Eukaryotic cells have coordinated systems to respond to DNA damage, such as cell cycle arrest mechanisms, DNA repair pathways and the apoptotic response. Together, these maintain genomic integrity (Sancar *et al*, 2004). These systems are partly regulated by transcriptional activation and repression (Zhan *et al*, 1993; Engelberg *et al*, 1994). We and others have recently identified histone H3-Thr 11 phosphorylation (H3-pThr 11) as a new transcriptional marker (Metzger *et al*, 2008; Shimada & Nakanishi, 2008; Shimada *et al*, 2008) that rapidly decreases after DNA damage. Under normal conditions Chk1 associates with chromatin (Smits *et al*, 2006; Niida *et al*, 2007) and phosphorylates H3-Thr 11. In response to DNA damage, Chk1 is rapidly released from chromatin and H3-pThr 11 is reduced.

[1]Department of Cell Biology, and
[2]Developmental and Regenerative Biology, Graduate School of Medical Sciences, Nagoya City University, 1 Kawasumi, Mizuho-cho, Mizuho-ku, Nagoya 467-8601, Japan
[+]Corresponding author. Tel: +81 52 853 8144; Fax: +81 52 842 3955;
E-mail: mkt-naka@med.nagoya-cu.ac.jp

Received 29 April 2010; revised 31 August 2010; accepted 31 August 2010; published online 15 October 2010

Mammalian serine (Ser)/threonine (Thr)-specific protein phos phatases (PPs) are represented by eight distinct prototypes: PP1, PP2A, PP2B, PP2C, PP4, PP5, PP6 and PP7 (Moorhead *et al*, 2007; Swingle *et al*, 2007). Of these, PP1, PP2A and PP4 have all been identified as histone phosphatases: PP1 dephosphorylates H1, which is phosphorylated in a cell-cycle-dependent manner (Paulson *et al*, 1996). The PP1 homologue dephosphorylates H3-pSer 10 at mitotic exit in yeast and worms (Hsu *et al*, 2000), and PP2A contributes to its dephosphorylation in *Drosophila* (Nowak *et al*, 2003). Phospho-H2AX (γ-H2AX) is immediately dephosphorylated after DNA repair by PP2A and PP4 in mammals and yeasts (Chowdhury *et al*, 2005, 2008; Keogh *et al*, 2006; Nakada *et al*, 2008). However, the phosphatases that catalyse H3-pThr 11 dephosphorylation in response to DNA damage have yet to be identified. In this study, we identify PP1γ as a phosphatase responsible for DNA-damage-induced dephosphorylation of H3-pThr 11.

RESULTS AND DISCUSSION

Dephosphorylation of pThr 11 is okadaic acid sensitive

To identify phosphatases that might be capable of DNA-damage-induced dephosphorylation of H3-pThr 11, we treated HeLa cells with different concentrations of okadaic acid (OA) and examined the status of H3-pThr 11 after ultraviolet (UV) irradiation. H3-pThr 11 was reduced after UV irradiation as previously reported (Shimada *et al*, 2008). Treatment with ⩾25 nM OA resulted in an increase in H3-pThr 11 in the absence of UV, making it difficult to evaluate the effect of OA treatment on DNA-damage-induced dephosphorylation of H3-pThr 11 (Fig 1A). We have previously reported that H3-pThr 11 is strongly enhanced at mitosis (Shimada *et al*, 2008). To establish whether the induction of H3-pThr 11 on OA treatment simply reflected an increase in the number of mitotic cells, we stained OA-treated cells with 4′,6-diamidino-2-phenylindole (DAPI) and calculated the mitotic index (Fig 1B). The mitotic index value increased more than threefold after OA treatment. However, in interphase cells, H3-pThr 11 is detected throughout the nuclear region with some exclusion of the peri-centromeric heterochromatin foci (represented by DAPI foci in Fig 1C). By contrast, at mitosis, strong

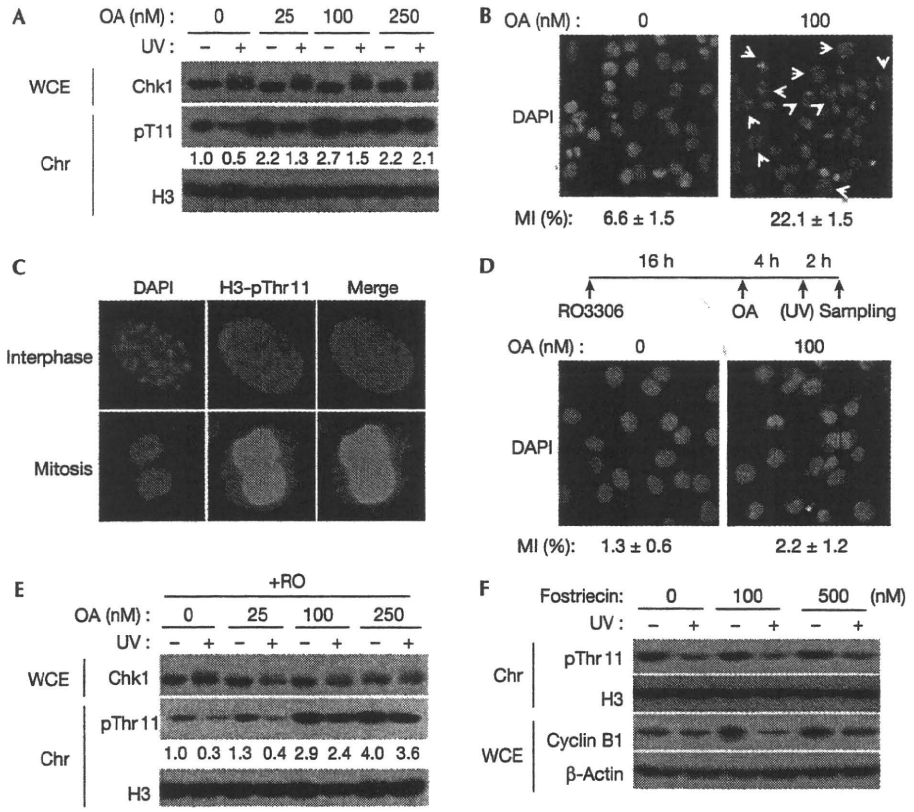

Fig 1 | The phosphatase responsible for H3-pThr11 dephosphorylation is sensitive to okadaic acid. (**A**) HeLa cells were pre-treated with the indicated concentrations of OA for 4 h. After irradiation with (+) or without (−) 100 J/m^2 UV, cells were cultured for an additional 2 h in the medium containing OA. WCE and Chr fractions were subjected to immunoblotting using the indicated antibodies. H3-pThr11 was quantified using NIH Image 1.62 Software and normalized relative to the total H3. The results were expressed at the bottom of the second panel as relative levels of H3-pThr11 compared with non-treated samples (0 h). (**B**) HeLa cells were fixed after the 6 h incubation with the indicated concentrations of OA and were stained with DAPI. The mitotic index (MI) indicates the percentage of cells with condensed chromosomes. Data are shown as means ± s.d. of four independent experiments. White arrowheads indicate mitotic cells. (**C**) MEFs were double-stained with H3-pThr11 antibodies and DAPI. Typical staining patterns of H3-pThr11 at interphase and mitosis are shown. (**D**) A scheme of the experimental strategy using HeLa cells and the MIs expressed as in (**B**) are shown. RO3306, 9 μM; OA, 100 nM. (**E**) HeLa cells irradiated with UV according to the strategy shown in (**D**) were collected, and WCE and Chr fractions were analysed by immunoblotting using the indicated antibodies. H3-pThr11 was quantified as in (**A**) and the results are shown at the bottom of the second panel. (**F**) HeLa cells incubated with fostriecin for 48 h were treated with (+) or without (−) UV. After 2 h incubation, WCE and chromatin fractions were subjected to immunoblotting. Chr, chromatin; DAPI, 4′,6-diamidino-2-phenylindole; MEF, mouse embryonic fibroblast; MI, mitotic index; NIH, National Institutes of Health; OA, okadaic acid; UV, ultraviolet; WCE, whole-cell extracts.

signals for H3-pThr11 are detected in condensed chromosomes, as reported previously (Preuss *et al*, 2003).

To evaluate the precise effect of OA treatment on H3-pThr11 independent of mitotic entry, we concomitantly treated cells with RO3306. Treatment with 9 μM RO3306 preferentially inhibits Cdk1 and thus prevents mitotic entry (Vassilev *et al*, 2006). The OA treatment did not result in an increase in the number of mitotic cells in the presence of 9 μM RO3306 (Fig 1D). Cell cycle arrest at G2 phase was induced as expected (supplementary Fig S1 online). DNA-damage-induced H3-pThr11 dephosphorylation was obvious at <100 nM OA, but almost completely abrogated at ≧100 nM OA in the presence of RO3306 when bands responsible for H3-pThr11 were quantified (Fig 1E). We observed that dephosphorylation of H3-pThr11 was not reduced after DNA damage, even at concentrations of 500 nM fostriecin—a specific inhibitor of PP2A—and its closely related PP4 and PP6 isotypes (Walsh *et al*, 1997; Fig 1F). At 100 nM, cyclin B1 had accumulated, demonstrating that inhibition was effective (Cheng *et al*, 1998). These results suggest that PP2A and its related phosphatases are not involved in DNA-damage-induced dephosphorylation of H3-pThr11.

PP1γ is a H3-pThr11 phosphatase

The OA sensitivity and fostriecin insensitivity in DNA-damage-induced dephosphorylation of H3-pThr11 suggested that the corresponding phosphatase might be a PP1 family member. We depleted PP1 by the using small interfering RNA (siRNA) that could suppress the expression of all three isoforms (PP1α, PP1β/δ and PP1γ) equally. Cells were treated with control, PP1 or PP2A siRNAs for 36 h in the presence of 0.5 mM hydroxyurea,

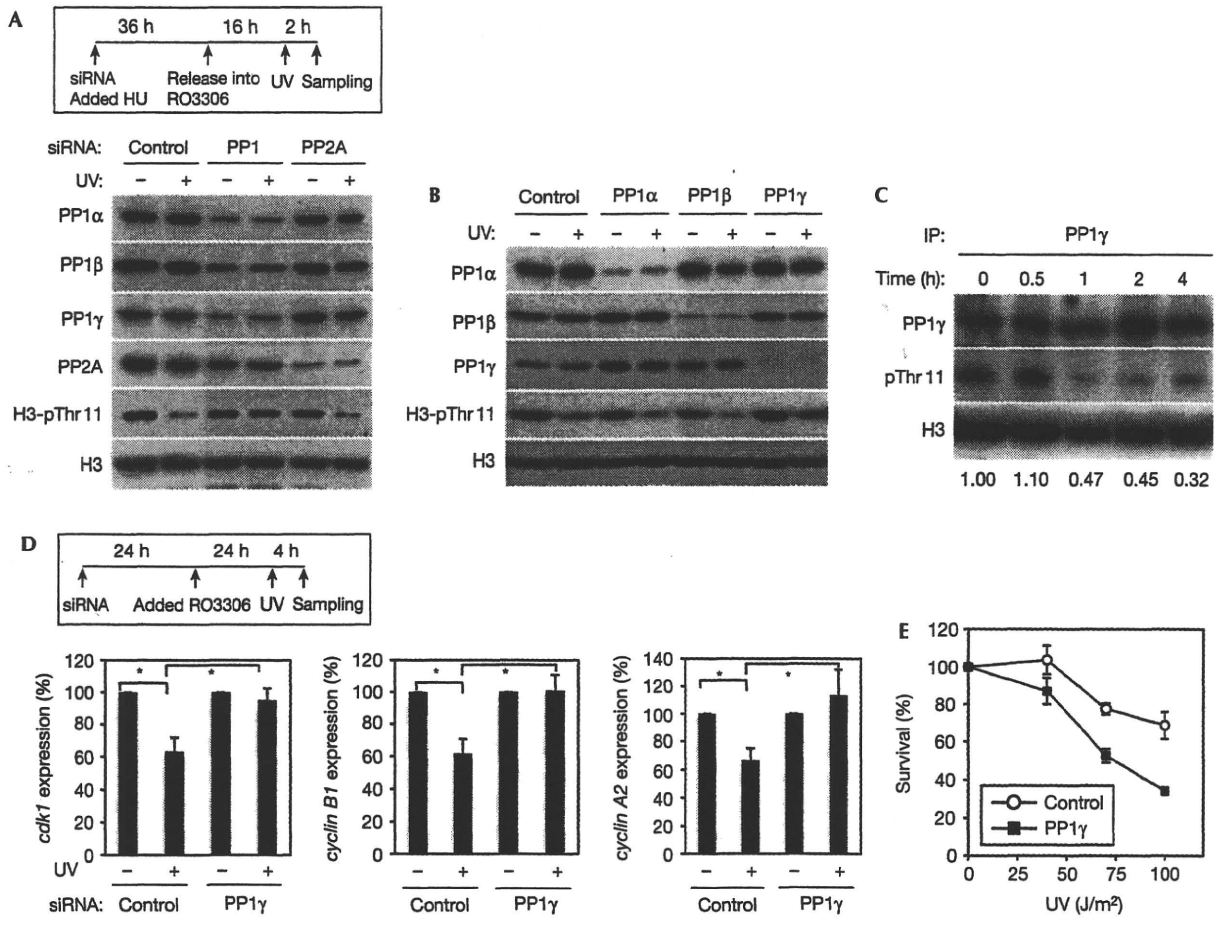

Fig 2 | Protein phosphatase 1γ is responsible for DNA-damage-induced dephosphorylation of H3-pThr11. (A) The experimental strategy is shown (upper panel). Whole-cell extracts with (+) or without (−) 100 J/m² UV were subjected to immunoblotting. **(B)** HCT116 cells were transfected with control, PP1 or PP2A siRNAs. After 70 h, cells were treated with (+) or without (−) 100 J/m² UV. After 2 h incubation, cells were collected and whole-cell extracts were subjected to immunoblotting. **(C)** MEFs were exposed to UV (100 J/m²) irradiation and collected at the indicated times. Endogenous PP1γ on the chromatin fraction was immunoprecipiated and the precipitates were subjected to immunoblotting and to an *in vitro* phosphatase assay using chromatin as a substrate. Phosphatase activity was examined by using immunoblotting with H3-pThr11 antibodies. H3-pThr11 was quantified and normalized relative to the total H3 as described in Fig 1E. The results are expressed as relative levels of H3-pThr11 compared with non-treated samples (0 h). **(D)** The experimental strategy is shown (upper panel). Total RNAs were prepared from HCT116 cells and quantitative real-time RT–PCR was performed using a set of primers within *cdk1*, *cyclin B1 and cyclin A2* transcripts. $^*P<0.003$. **(E)** HCT116 cells transfected with control or PP1γ siRNAs for 72 h in 96-well plates were irradiated with UV (0, 40, 70 and 100 J/m²). The cell viability was determined 72 h after UV by MTT assay as described in the Methods section. The results were expressed as the percentage ratio of non-irradiated cells. MEF, mouse embryonic fibroblast; MTT, 3-(4,5-dimethylthiazol-2-y1)-2,5-diphenyltetrazolium bromide; PP, protein phosphatase; RT–PCR, reverse transcriptase PCR; siRNA, small interfering RNA; UV, ultraviolet.

which prevents mitotic arrest by PP1 or PP2A depletion. After 36 h, cells were released from hydroxyurea arrest and incubated with RO3306 for 16 h. Finally, cells were irradiated with UV and sampled 2 h later (Fig 2A, upper panel). The depletion of PP1, but not of PP2A, resulted in compromised H3-pThr11 dephosphorylation after UV (Fig 2A).

We further demonstrated that PP1γ depletion specifically compromised DNA-damage-induced H3-pThr11 dephosphorylation in both HCT116 (Fig 2B) and HeLa (supplementary Fig S2A,B online) cells. Depletion of individual PP1 subunits did not result in gross changes in cell cycle distribution, although PP1γ depletion mitotic index resulted in a slight increase in the mitotic index value (supplementary Fig S3 online). It is interesting to note that PP1γ phosphatase activity towards H3-pThr11 was activated as early as 1 h and maintained for up to 4 h after DNA damage (Fig 2C). Changes in the expression of cell cycle regulatory genes after PP1γ depletion were examined in cells treated with RO3306 to prevent low-level induction of mitotic cells. Treatment with RO3306 did not affect the expression of these genes (supplementary Table S1 online). The depletion of PP1γ suppressed DNA-damage-induced transcriptional repression of *cdk1*, *cyclin B1* and *cyclin A2* (Fig 2D). Importantly, PP1γ depletion sensitized HCT 116 cells to UV when cell survival was evaluated by MTT (3-[4,5-dimethylthiazol-2-y1]-2,5-diphenyltetrazolium bromide)

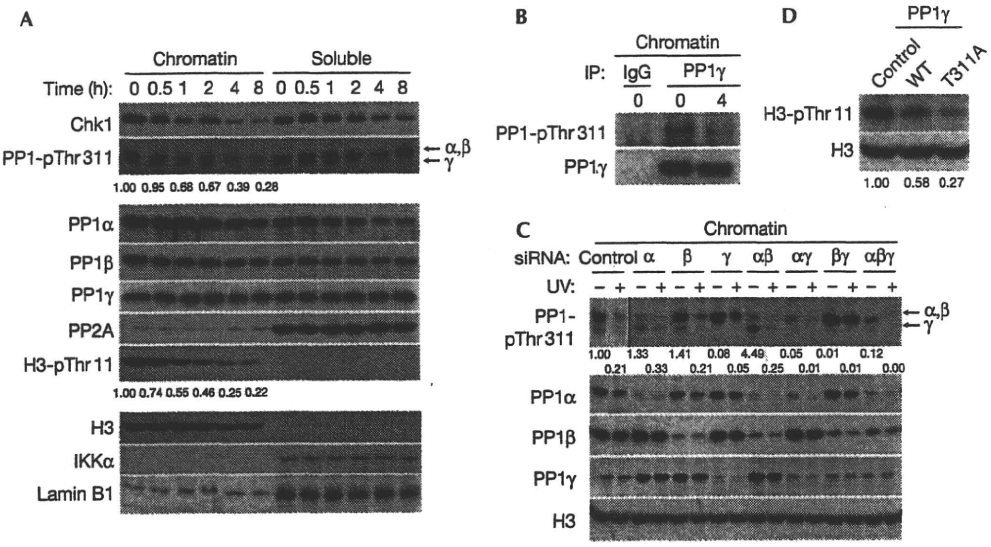

Fig 3 | Protein phosphatase 1γ-pThr 311 on chromatin is decreased after DNA damage. (**A**) HCT116 cells were treated with UV (100 J/m^2) and collected at the indicated times. The chromatin and soluble fractions were subjected to immunoblotting using the indicated antibodies. IKKα and lamin B1 were used as markers of soluble proteins. PP1γ-pThr 311 and H3-pThr 11 were quantified and normalized relative to the total PP1γ and H3, respective. The results are expressed at the bottom of the second and seventh panels as relative levels of PP1γ-pThr 311 and H3-pThr 11 compared with non-treated samples (0 h). (**B**) Chromatin fractions from UV-irradiated HCT116 cells were solubilized and subjected to IP-western analysis using the indicated antibodies. (**C**) To separate the isoforms of PP1 by SDS–PAGE, chromatin fractions from cells depleted of the indicated PP1 isoforms with (+) or without (−) UV were subjected to immunoblotting using an SDS–PAGE gel containing 10 μM Phos Tag. Arrows indicate bands corresponding to PP1α, β and γ isoforms. PP1γ-pThr 311 was quantified and the results were expressed at the bottom of the first panel as relative levels of PP1γ-pThr 311 compared with control (−UV). (**D**) The wild type or the T311A mutant of His-PP1γ purified from Sf9 cells were incubated with chromatin from HCT116 cells for 1 h at 30 °C. The status of H3-pThr 11 was monitored by immunoblotting using H3-pThr 11 antibodies. H3-pThr 11 was quantified and normalized relative to the total H3. The results are expressed at the bottom of the second panel as relative levels of H3-pThr 11 compared with the control sample. IKKα, IkB kinase α; IP, immunoprecipitation; PP, protein phosphatase; SDS–PAGE, sodium dodecyl sulphate–polyacrylamide gel electrophoresis; UV, ultraviolet.

assay (Fig 2E), suggesting the physiological importance of PP1γ-dependent transcriptional repression after DNA damage. Although the molecular mechanism by which PP1γ regulates H3-pThr 11 dephosphorylation after DNA damage has remained elusive, isoform-specific functions for PP1 have been reported in the regulation of SRp38 dephosphorylation (Shi & Manley, 2007) and in the control of chromosomal architecture (Trinkle-Mulcahy *et al*, 2006).

Regulation of PP1γ activity in response to DNA damage

The activity of PP1α is reported to be downregulated by Cdk-dependent Thr320 phosphorylation (Dohadwala *et al*, 1994). The equivalent threonine residue is conserved in all three PP1 isoforms (Thr316 in PP1β/δ and Thr311 in PP1γ). Indeed, cyclin B1–Cdk1-phosphorylated PP1γ-Thr311 *in vitro* (supplementary Fig S4A online). Cdk activity is strongly inhibited after DNA damage, in a manner dependent on Chk1 (Harper & Elledge, 2007). We therefore examined changes in the phosphorylation status of PP1 subunits after UV irradiation by using a combination of isoform-specific antibodies and a phospho-specific Thr320 (PP1α) antibody (Fig 3A). All PP1 isoforms were similarly localized in both chromatin and soluble fractions of HCT116 cells. As a control, IkB kinase α (IKKα)—a typical cytosolic protein—and lamin B1—a marker of the nuclear soluble fraction—were predominantly detected in the soluble fraction, indicating that the subcellular fractionation was successful. The PP1-pThr 320-specific signal for each isoform was rapidly dephosphorylated in response to UV, particularly in the chromatin fraction, with kinetics that were similar to that of H3-pThr 11. As the PP1α-pThr 320-specific antibody can recognize the corresponding phosphorylations of PP1β/δ and PP1γ, we further examined whether PP1γ-pThr 311 was dephosphorylated after UV treatment. We observed that PP1γ-pThr 311 in PP1γ immune complexes was reduced (Fig 3B). We separated the three isoforms of PP1 using sodium dodecyl sulphate–polyacrylamide gel electrophoresis containing Phos Tag (Kinoshita *et al*, 2009). Treatment of HCT116 cells with each isoform-specific siRNA or their combinations revealed that PP1γ migrated fastest, followed by PP1α and PP1β (Fig 3C), although the amounts of each isoform and their phosphorylations at Thr311 were induced after depletion of the other isoforms, presumably due to a compensatory mechanism. The PP1γ-pThr 311-specific signal was consistently decreased in response to UV irradiation when bands responsible for PP1γ-pThr 311 were quantified. Similar kinetics were observed when cells were treated with bleomycin (supplementary Fig S4B online) or ionizing radiation (supplementary Fig S4C online), and the extent of PP1γ-pThr 311 dephosphorylation was found to be dependent on the UV dose (supplementary Fig S4D online). Importantly, the phosphorylation-defective mutant of PP1γ (T311A) was more active *in vitro* than in the wild-type PP1γ (Fig 3D).

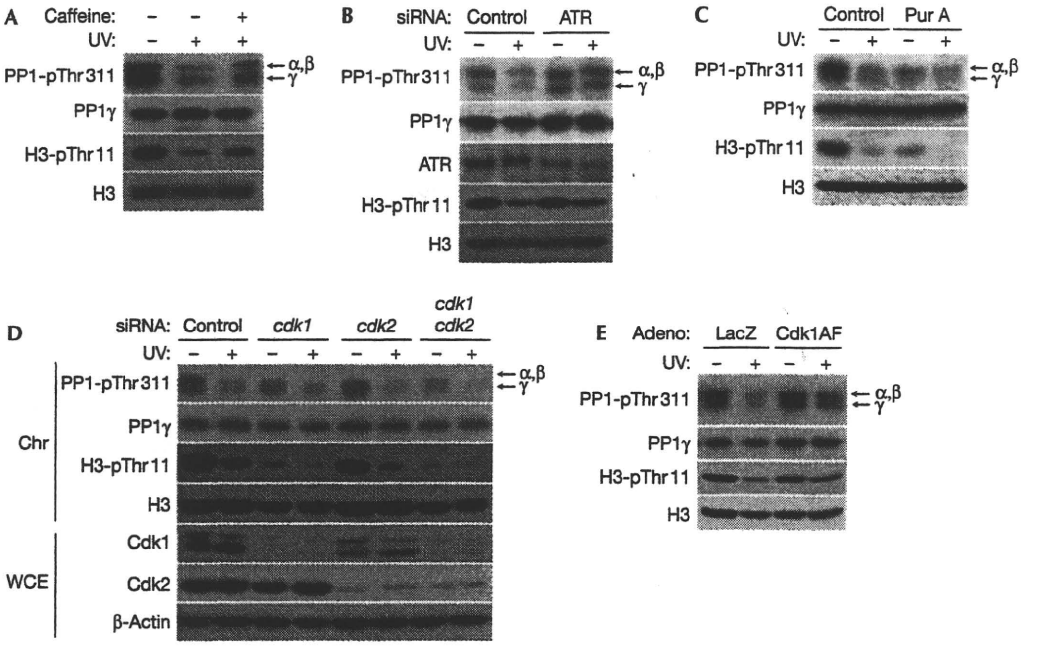

Fig 4 | Cdk-dependent phosphorylation of protein phosphatase 1γ at Thr311 is involved in DNA-damage-induced transcriptional repression. (**A**) HCT116 cells were pre-incubated in the presence (+) or absence (−) of 5 mM caffeine for 4 h and then treated with (+) or without (−) UV (100 J/m²). Cells were collected 2 h after UV treatment and their chromatin fractions were analysed by immunoblotting using the indicated antibodies. (**B**) HCT116 cells were transfected with control or ATR siRNAs. After 70 h, cells were treated with (+) or without (−) UV (100 J/m²) and incubated for an additional 4 h. Chromatin fractions were analysed by immunoblotting. (**C**) HCT116 cells were treated with 10 μM purvalanol A for 22 h, irradiated with UV (100 J/m²) and incubated for an additional 4 h. The chromatin fractions were analysed by immunoblotting. (**D**) HCT116 cells were transfected with control, *cdk1* and/or *cdk2* siRNAs. After 70 h, cells were treated with (+) or without (−) UV (100 J/m²) and incubated for an additional 4 h. The chromatin fractions or WCE were analysed by immunoblotting using the indicated antibodies. (**E**) HCT116 cells were infected with adenoviruses expressing LacZ as a control or the constitutively active Cdk1 mutant (Cdk1AF), and treated with (+) or without (−) UV (100 J/m²) 24 h after infection. Cells were collected 4 h after UV treatment and their chromatin fractions were analysed by immunoblotting using the indicated antibodies. ATR, ataxia telangiectasia, mutated and Rad3-related; Chr, chromatin; PP, protein phosphatase; siRNA, small interfering RNA; UV, ultraviolet; WCE, whole-cell extracts.

ATR–Chk1 axis regulates PP1γ activity

Treatment with caffeine—an inhibitor of the ataxia telangiectasia, mutated and Rad3-related (ATR) and ataxia telangiectasia, mutated kinases—partly suppressed DNA-damage-dependent dephosphorylation of PP1γ-pThr311 (Fig 4A). The knockdown of ATR by siRNA compromised UV-dependent PP1γ-pThr311 dephosphorylation (Fig 4B). Treatment with purvalanol A, a specific Cdk inhibitor, resulted in almost complete reduction in PP1γ-pThr311 and H3-pThr11 in the absence of DNA damage (Fig 4C). Both PP1γ-pThr311 and H3-pThr11 were significantly reduced when Cdk1 was depleted, and further reduced when both Cdk1 and Cdk2 were depleted (Fig 4D). By contrast, ectopic expression of a constitutively active Cdk1 mutant (Cdk1AF) inhibited UV-induced dephosphorylation of PP1γ-pThr311 and H3-pThr11 (Fig 4E). These results suggest that ATR/Chk1-dependent inhibition of Cdk activity results in dephosphorylation of PP1γ-pThr311 and activation of PP1γ, leading to dephosphorylation of H3-pThr11 (Fig 5).

In this study, we demonstrate that the dephosphorylation of H3-pThr11 and the subsequent transcriptional repression of cell cycle regulatory genes after DNA damage are regulated at least in part by the ATR–Chk1–Cdk–PP1γ axis. This pathway seems to have an important role in cell survival after DNA damage. Although the precise mechanism by which PP1γ regulates cell viability remains unknown, levels of cyclins and Cdks might be a crucial determinant of cell viability after DNA damage.

METHODS

Cell culture and adenovirus infection. HCT116 cells were cultured in McCoy's 5a medium containing 10% fetal bovine serum. HeLa cells and mouse embryonic fibroblasts were cultured in Dulbecco's modified Eagle medium containing 10% fetal bovine serum. All cells were cultured at 37 °C in 5% CO_2. Adenovirus-Cdk1AF (Niida *et al*, 2005) or LacZ (control) was used to infect HCT116 cells at multiplicity of infection 40.

Immunoblotting. Subcellular fractionation was performed as previously described (Niida *et al*, 2007). To solubilize the chromatin fraction, pellets were suspended in immunoprecipitation kinase buffer (50 mM HEPES (pH 8.0), 150 mM NaCl, 2.5 mM EGTA, 1 mM dithiothreitol, 0.1% Tween-20, 10% glycerol and protease inhibitors). For preparation of whole-cell extracts, cells were lysed in immunoprecipitation kinase buffer.

Phosphatase assay. Chromatin-bound PP1γ was solubilized and immunoprecipitated with PP1γ antibody. The precipitates were

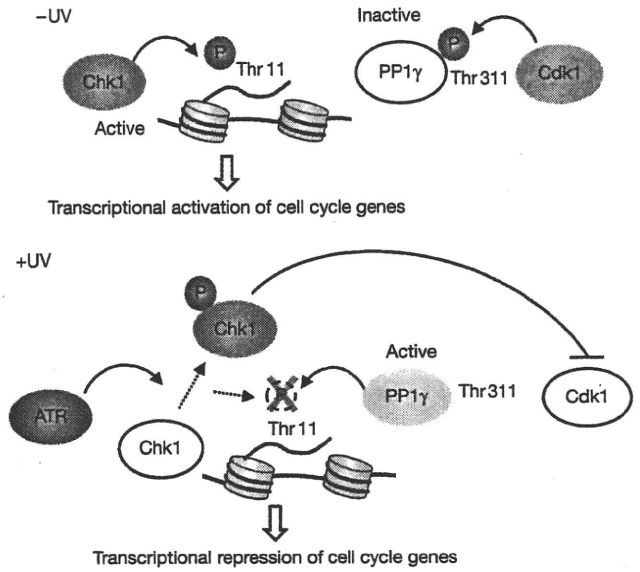

Fig 5 | Schematic model of DNA-damage-induced dephosphorylation of H3-pThr11 on the promoters of cell cycle regulatory genes. Under normal conditions (−UV), Chk1 associates with chromatin and phosphorylates H3-Thr11 to activate transcription of cell cycle regulatory genes. PP1γ is inactivated through Cdk-dependent phosphorylation at Thr311. In response to DNA damage (+UV), activated ATR phosphorylates Chk1 and the phosphorylated Chk1 then dissociates from chromatin. ATR-dependent release of Chk1 from the promoters of cell cycle regulatory genes indirectly suppresses Cdk activity, which results in activation of PP1γ through a reduction in Thr311 phosphorylation. PP1γ-mediated dephosphorylation of H3-pThr11 represses transcription of genes involved in cell cycle regulation. ATR, ataxia telangiectasia, mutated and Rad3-related; PP, protein phosphatase; UV, ultraviolet.

incubated with chromatin at 30 °C for 1 h in phosphatase buffer (10 mM HEPES, 10 mM $MgCl_2$, 1 mM $MnCl_2$ and 1 mM DTT). His-tagged wild-type PP1γ or PP1γ-Thr311A was purified from Sf9 cells and phosphatase assays were performed using a chromatin fraction as a substrate.

Knockdown experiments by siRNA transfection. HCT116 or HeLa cells were transfected with either a control siRNA (Silencer Negative Control, Ambion) or an siRNA for ATR, PP1, PP1α, PP1β, PP1γ, PP2A or Cdk1 and Cdk2 using Lipofectamine 2000 (Invitrogen). The sequences of these siRNAs were described in the supplementary Table S2 online.

Immunofluorescence. Cells were grown on glass coverslips or chamber slides, washed with phosphate buffered saline (PBS) and fixed with 2% paraformaldehyde in PBS for 15 min, and stained with the indicated antibodies diluted in 5% blocking buffer (Convance, normal serum block) and DAPI.

Quantitative real-time RT–PCR for measurement of *Cdk1*, *cyclin B1* and *cyclin A2* mRNA expressions. The RNA was extracted using ISOGEN (Wako) according to the manufacturer's protocol. Total RNAs were subjected to reverse transcription. *Cdk1*, *cyclin B1* and *cyclin A2* mRNA levels were measured by Taqman quantitative PCR, normalized to *GAPDH* gene expression and expressed relative to the un-irradiated sample.

MTT assay. HCT116 cells were incubated with medium containing MTT solution (0.5 mg/ml) for 4 h. After removing the medium, cells were incubated with DMSO and the optical density of the resultant supernatant was measured at 535 nm.

Antibodies. The antibodies used for immunoblotting were ATR (sc-1887; Santa Cruz Biotechnology), β-actin (ab6276; Abcam), Chk1 (sc-8408 and sc-56291; Santa Cruz Biotechnology), Myc (sc-789 and sc-40; Santa Cruz Biotechnology), Cdk1 (sc-54; Santa Cruz Biotechnology), Cdk2 (sc-163; Santa Cruz Biotechnology), FLAG (M2; Sigma), H3 (ab1791; Abcam), IKKα (sc-7182; Santa Cruz Biotechnology), H3 (9715; Cell Signaling Technology), pT11 (ab5168; Abcam), PP1 (sc-7482; Santa Cruz Biotechnology), pThr320-PP1 (2581; Cell Signaling Technology), PP2A (05-421; Upstate), PP1α (06-221; Upstate), PP1β (ab53315; Abcam) and PP1γ (sc-6108; Santa Cruz Biotechnology, 07-1298; Millipore).

Supplementary information is available at EMBO *reports* online (http://www.emboreports.org).

ACKNOWLEDGEMENTS

We thank P.M. Carr, D. Zineldeen and M. Delhase for critical reading of this paper; and Y. Chiba, S. Tsubaki, Y. Kawada, T. Misaki, Y. Koshiyama and C. Yamada-Namikawa for technical assistance. This study was supported in part by a Grant-in-Aid for Scientific Research (B) and the project for realization of regenerative medicine, by the Mitsubishi Foundation, by the Naito Memorial Foundation and by the Toyoaki Foundation (to M.N.), by the Mochida Memorial Foundation, Shiseido Female Researcher Science Grant and by a Grant-in-Aid for Young Scientists (A; to M.S.).

CONFLICT OF INTEREST

The authors declare that they have no conflict of interest.

REFERENCES

Cheng A, Balczon R, Zuo Z, Koons JS, Walsh AH, Honkanen RE (1998) Fostriecin-mediated G2–M-phase growth arrest correlates with abnormal centrosome replication, the formation of aberrant mitotic spindles, and the inhibition of serine/threonine protein phosphatase activity. *Cancer Res* **58:** 3611–3619

Chowdhury D, Keogh MC, Ishii H, Peterson CL, Buratowski S, Lieberman J (2005) γ-H2AX dephosphorylation by protein phosphatase 2A facilitates DNA double-strand break repair. *Mol Cell* **20:** 801–809

Chowdhury D, Xu X, Zhong X, Ahmed F, Zhong J, Liao J, Dykxhoorn DM, Weinstock DM, Pfeifer GP, Lieberman J (2008) A PP4-phosphatase complex dephosphorylates γ-H2AX generated during DNA replication. *Mol Cell* **31:** 33–46

Dohadwala M, da Cruz e Silva EF, Hall FL, Williams RT, Carbonaro-Hall DA, Nairn AC, Greengard P, Berndt N (1994) Phosphorylation and inactivation of protein phosphatase 1 by cyclin-dependent kinases. *Proc Natl Acad Sci USA* **91:** 6408–6412

Engelberg D, Klein C, Martinetto H, Struhl K, Karin M (1994) The UV response involving the Ras signaling pathway and AP-1 transcription factors is conserved between yeast and mammals. *Cell* **77:** 381–390

Harper JW, Elledge SJ (2007) The DNA damage response: ten years after. *Mol Cell* **28:** 739–745

Hsu JY *et al* (2000) Mitotic phosphorylation of histone H3 is governed by Ipl1/aurora kinase and Glc7/PP1 phosphatase in budding yeast and nematodes. *Cell* **102:** 279–291

Keogh MC *et al* (2006) A phosphatase complex that dephosphorylates γH2AX regulates DNA damage checkpoint recovery. *Nature* **439:** 497–501

Kinoshita E, Kinoshita-Kikuta E, Koike T (2009) Separation and detection of large phosphoproteins using Phos-tag SDS–PAGE. *Nat Protoc* **4:** 1513–1521

Metzger E *et al* (2008) Phosphorylation of histone H3 at threonine 11 establishes a novel chromatin mark for transcriptional regulation. *Nat Cell Biol* **10:** 53–60

Moorhead GB, Trinkle-Mulcahy L, Ulke-Lemee A (2007) Emerging roles of nuclear protein phosphatases. *Nat Rev Mol Cell Biol* **8:** 234–244

Nakada S, Chen GI, Gingras AC, Durocher D (2008) PP4 is a γH2AX phosphatase required for recovery from the DNA damage checkpoint. *EMBO Rep* **9:** 1019–1026

Niida H, Tsuge S, Katsuno Y, Konishi A, Takeda N, Nakanishi M (2005) Depletion of Chk1 leads to premature activation of Cdc2–cyclin B and mitotic catastrophe. *J Biol Chem* **280:** 39246–39252

Niida H, Katsuno Y, Banerjee B, Hande MP, Nakanishi M (2007) Specific role of Chk1 phosphorylations in cell survival and checkpoint activation. *Mol Cell Biol* **27:** 2572–2581

Nowak SJ, Pai CY, Corces VG (2003) Protein phosphatase 2A activity affects histone H3 phosphorylation and transcription in *Drosophila melanogaster*. *Mol Cell Biol* **23:** 6129–6138

Paulson JR, Patzlaff JS, Vallis AJ (1996) Evidence that the endogenous histone H1 phosphatase in HeLa mitotic chromosomes is protein phosphatase 1, not protein phosphatase 2A. *J Cell Sci* **109:** 1437–1447

Preuss U, Landsberg G, Scheidtmann KH (2003) Novel mitosis-specific phosphorylation of histone H3 at Thr11 mediated by Dlk/ZIP kinase. *Nucleic Acids Res* **31:** 878–885

Sancar A, Lindsey-Boltz LA, Unsal-Kacmaz K, Linn S (2004) Molecular mechanisms of mammalian DNA repair and the DNA damage checkpoints. *Annu Rev Biochem* **73:** 39–85

Shi Y, Manley JL (2007) A complex signaling pathway regulates SRp38 phosphorylation and pre-mRNA splicing in response to heat shock. *Mol Cell* **28:** 79–90

Shimada M, Nakanishi M (2008) Checkpoints meet the transcription at a novel histone milestone (H3-T11). *Cell Cycle* **7:** 1555–1559

Shimada M, Niida H, Zineldeen DH, Tagami H, Tanaka M, Saito H, Nakanishi M (2008) Chk1 is a histone H3 threonine 11 kinase that regulates DNA damage-induced transcriptional repression. *Cell* **132:** 221–232

Smits VA, Reaper PM, Jackson SP (2006) Rapid PIKK-dependent release of Chk1 from chromatin promotes the DNA-damage checkpoint response. *Curr Biol* **16:** 150–159

Swingle M, Ni L, Honkanen RE (2007) Small-molecule inhibitors of Ser/Thr protein phosphatases: specificity, use and common forms of abuse. *Methods Mol Biol* **365:** 23–38

Trinkle-Mulcahy L, Andersen J, Lam YW, Moorhead G, Mann M, Lamond AI (2006) Repo-Man recruits PP1γ to chromatin and is essential for cell viability. *J Cell Biol* **172:** 679–692

Vassilev LT, Tovar C, Chen S, Knezevic D, Zhao X, Sun H, Heimbrook DC, Chen L (2006) Selective small-molecule inhibitor reveals critical mitotic functions of human CDK1. *Proc Natl Acad Sci USA* **103:** 10660–10665

Walsh AH, Cheng A, Honkanen RE (1997) Fostriecin, an antitumor antibiotic with inhibitory activity against serine/threonine protein phosphatases types 1 (PP1) and 2A (PP2A), is highly selective for PP2A. *FEBS Lett* **416:** 230–234

Zhan Q, Carrier F, Fornace Jr AJ (1993) Induction of cellular p53 activity by DNA-damaging agents and growth arrest. *Mol Cell Biol* **13:** 4242–4250

The EMBO Journal (2010) 29, 3558–3570 | © 2010 European Molecular Biology Organization | All Rights Reserved 0261-4189/10
www.embojournal.org

THE EMBO JOURNAL

Cooperative functions of Chk1 and Chk2 reduce tumour susceptibility *in vivo*

Hiroyuki Niida[1,7], Kazuhiro Murata[1], Midori Shimada[1], Kumiko Ogawa[2], Kumiko Ohta[3], Kyoko Suzuki[3], Hidetsugu Fujigaki[4], Aik Kia Khaw[5], Birendranath Banerjee[5], M Prakash Hande[5], Tomomi Miyamoto[6], Ichiro Miyoshi[6], Tomoyuki Shirai[2], Noboru Motoyama[3], Mireille Delhase[1], Ettore Appella[4] and Makoto Nakanishi[1,*]

[1]Department of Cell Biology, Nagoya City University, Kawasumi, Mizuho-cho, Mizuho-ku, Nagoya, Japan, [2]Department of Experimental Pathology and Tumor Biology, Nagoya City University, Kawasumi, Mizuho-cho, Mizuho-ku, Nagoya, Japan, [3]Department of Cognitive Brain Science, National Center for Geriatrics and Gerontology, Obu, Aichi, Japan, [4]Laboratory of Cell Biology, National Cancer Institute, National Institutes of Health, Bethesda, MD, USA, [5]Department of Physiology, Yong Loo Lin School of Medicine, National University of Singapore, Singapore, Singapore, [6]Department of Comparative and Experimental Medicine and Center for Animal Science, Graduate School of Medical Sciences, Nagoya City University, Kawasumi, Mizuho-cho, Mizuho-ku, Nagoya, Japan and [7]Department of Biochemistry, Hamamatsu University School of Medicine, Handayama, Higashi-ku, Hamamatsu, Shizuoka, Japan

Although the linkage of Chk1 and Chk2 to important cancer signalling suggests that these kinases have functions as tumour suppressors, neither *Chk1*$^{+/-}$ nor *Chk2*$^{-/-}$ mice show a predisposition to cancer under unperturbed conditions. We show here that *Chk1*$^{+/-}$*Chk2*$^{-/-}$ and *Chk1*$^{+/-}$ *Chk2*$^{+/-}$ mice have a progressive cancer-prone phenotype. Deletion of a single *Chk1* allele compromises G2/M checkpoint function that is not further affected by Chk2 depletion, whereas Chk1 and Chk2 cooperatively affect G1/S and intra-S phase checkpoints. Either or both of the kinases are required for DNA repair depending on the type of DNA damage. Mouse embryonic fibroblasts from the double-mutant mice showed a higher level of p53 with spontaneous DNA damage under unperturbed conditions, but failed to phosphorylate p53 at S23 and further induce p53 expression upon additional DNA damage. Neither Chk1 nor Chk2 is apparently essential for p53- or Rb-dependent oncogene-induced senescence. Our results suggest that the double Chk mutation leads to a high level of spontaneous DNA damage, but fails to eliminate cells with damaged DNA, which may ultimately increase cancer susceptibility independently of senescence.

The EMBO Journal (2010) **29**, 3558–3570. doi:10.1038/emboj.2010.218; Published online 10 September 2010

*Corresponding author. Department of Cell Biology, Graduate School of Medical Sciences, Nagoya City University, 1 Kawasumi, Mizuho-cho, Mizuho-ku, Nagoya, Aichi 467-8601, Japan. Tel.: +81 52 853 8144; Fax: +81 52 842 3955; E-mail: mkt-naka@med.nagoya-cu.ac.jp

Received: 2 April 2010; accepted: 10 August 2010; published online: 10 September 2010

Subject Categories: genome stability & dyanamics; molecular biology of disease
Keywords: apoptosis; cancer; checkpoint; DNA damage; senescence

Introduction

Aberrant regulation of DNA-damage response in multicellular organisms is thought to lead to genomic instability and cancer development (Bartkova *et al*, 2005; Gorgoulis *et al*, 2005). Signals initiated by DNA-damage sensors are rapidly transduced to ATM/ATR kinases that in turn phosphorylate a large number of substrates, including checkpoint kinases (Chks), Chk1 and Chk2. In cell culture-based systems, Chk1 and Chk2 behave similarly and appear to regulate activities involving the Cdc25 family of phosphatases (Sanchez *et al*, 1997; Matsuoka *et al*, 1998; Kaneko *et al*, 1999; Tominaga *et al*, 1999), p53 (Shieh *et al*, 2000) and DNA-repair factors (Lee *et al*, 2000; Sorensen *et al*, 2005). In knockout mice, however, the respective phenotypes are very different (Hirao *et al*, 2000; Liu *et al*, 2000; Takai *et al*, 2000, 2002), suggesting that these kinases regulate distinct pathways *in vivo*. In the light of the relationship between these checkpoint kinases and important cancer signalling pathways (Bartkova *et al*, 2005; Gorgoulis *et al*, 2005) and the genetic alterations of *Chk1* and *Chk2* observed in sporadic (Bertoni *et al*, 1999) and familial tumours (Bell *et al*, 1999; Bartek and Lukas, 2003), the lack of an overt tumour-prone phenotype in *Chk1* and *Chk2* knockout mice was somewhat unanticipated (Hirao *et al*, 2000; Liu *et al*, 2000; Takai *et al*, 2000, 2002). Interestingly, tumour incidence was increased in *Chk1*$^{+/-}$, *WNT-1* transgenic mice (Liu *et al*, 2000), *Chk2*$^{-/-}$*Brca1*$^{-/-}$ (McPherson *et al*, 2004), *Chk2*$^{-/-}$ *Brca1*$^{\Delta 11/\Delta 11}$ (Cao *et al*, 2006), *Chk2*$^{-/-}$*NBS1*$^{\Delta B/\Delta B}$ and *Chk2*$^{-/-}$ *Mre11*$^{ATLD1/ATLD1}$ mice (Stracker *et al*, 2008). This may be explained by the redundancy found in biochemical studies, which show that both kinases can phosphorylate the same sites on the same substrates, at least *in vitro*, and that either Chk1 or Chk2 is sufficient to mediate anti-tumour signalling. Alternatively, Chk1 and Chk2 may function in non-redundant DNA-damage response and either response is sufficient to prevent tumour formation *in vivo*.

In this respect, Lam *et al* (2004) showed that Chk1 haploinsufficiency could potentially have a tumour suppressor function. Inactivation of one *Chk1* allele showed inappropriate entry into S phase, accumulation of spontaneous DNA damage during DNA replication and a failure to restrain mitotic entry in the presence of a deregulated S phase. Nevertheless, inactivation of one *Chk1* allele *per se* did not lead to cancer predisposition. Thus, apparent cancer-related phenotypes in *Chk1*$^{+/-}$ cells might be suppressed in *in vivo* tumourigenesis through other DNA-damage responses. To address this critical question, a more exhaustive tumourigenesis study performed in double-mutant mice would be

necessary. This study clearly shows that Chk1 and Chk2 are bona fide and cooperatively haplo-insufficient tumour suppressors *in vivo* that regulate cell cycle checkpoints and apoptosis, but not premature senescence. Mice with the combined loss of two anti-tumour barriers are not able to eliminate cells with a high level of DNA damage and this may be sufficient for the predisposition to spontaneous tumourigenesis.

Results

Tumourigenesis in Chk1/Chk2 double-mutant mice

We generated $Chk1^{+/-}Chk2^{-/-}$ mice to conduct a systematic evaluation of the checkpoint kinase function *in vivo* because at least one *Chk1* allele is essential for survival and proliferation of both embryonic (Liu *et al*, 2000; Takai *et al*, 2000) and somatic cells (Shimada *et al*, 2008). Exhaustive characterization of mice bearing single or combined germline *Chk1* and *Chk2* deletions revealed that a significantly higher percentage of mice developed aggressive malignant lymphomas, sarcomas or lung adenomas in $Chk1^{+/-}Chk2^{-/-}$ mice (Figure 1A and B; HR = 19.2, 95% CI = 2.5–147.4, $P = 0.004$). Unexpectedly, $Chk1^{+/-}Chk2^{+/-}$ mice also showed a predisposition to cancer, bearing lymphomas, sarcomas or carcinomas (Figure 1C–H) (HR = 9.3, 95% CI = 1.2–74.3, $P = 0.035$), although tumour production occurred later than in $Chk1^{+/-}Chk2^{-/-}$ mice. Examination of $Chk1^{+/-}Chk2^{+/+}$ and $Chk1^{+/+}Chk2^{-/-}$ mice revealed no apparent cancer-prone phenotypes during this experimental period (Figure 1A and data not shown). We examined the lineage of lymphomas observed in $Chk1^{+/-}Chk2^{+/-}$ and $Chk1^{+/-}Chk2^{-/-}$ mice by immunostaining using antibodies to PAX5 as a B-cell marker and CD3 as a T-cell marker. Those lymphomas were positive for PAX5 and negative for CD3, indicating that they were from the B-cell lineage. The typical staining of those lymphomas is shown in Figure 1I.

We then examined whether Chk1 and Chk2 function as typical or haplo-insufficient tumour suppressors. Quantitative real-time PCR using cDNAs from tumour sections revealed that Chk1 was still expressed in tumours of $Chk1^{+/-}Chk2^{+/-}$ and $Chk1^{+/-}Chk2^{-/-}$ mice and Chk2 was also expressed in those of $Chk1^{+/-}Chk2^{+/-}$ mice (Figure 1J). These results suggest that both Chk1 and Chk2 are haplo-insufficient tumour suppressors. Aside from their striking cancer susceptibility, $Chk1^{+/-}Chk2^{-/-}$ mice were indistinguishable from their wild-type siblings. $Chk1^{-/-}Chk2^{-/-}$ mice, however, died at an early embryonic stage (Supplementary Table SI), indicating that Chk2 depletion failed to rescue embryonic lethality in $Chk1^{-/-}$ mice and suggesting that in mice a single *Chk1* allele is sufficient for normal embryonic development or post-natal life.

Aberrant cell cycle checkpoints in Chk1/Chk2 double-mutant cells

In order to characterize the tumourigenicity observed in $Chk1^{+/-}Chk2^{+/-}$ and $Chk1^{+/-}Chk2^{-/-}$ mice, we generated primary mouse embryonic fibroblasts (MEFs) from littermates obtained from double-heterozygote breeders. Our strategy to assess the immediate G1/S phase checkpoints after exposure to ionizing radiation (IR) involved staggered CIdU/IdU labelling. The labelling strategy is shown in Figure 2A (left panel). In this assay, single-labelled IdU cells are ones that entered S phase after IR, so this allowed us to evaluate initiation of the G1/S checkpoint without any effect from the intra-S phase checkpoint. Although irradiation reduced the proportion of IdU single-positive cells to 40% in $Chk1^{+/+}Chk2^{+/+}$ cells, those of $Chk1^{+/-}Chk2^{+/+}$ and $Chk1^{+/-}Chk2^{+/-}$ cells were only reduced to 67% ($P<0.05$) and 70% ($P<0.05$), respectively (Figure 2A). No reduction in S phase entry was observed in $Chk1^{+/+}Chk2^{-/-}$ and $Chk1^{+/-}Chk2^{-/-}$ cells. Thus, a synergistic effect on this checkpoint was observed by combined deletion of a single *Chk1* allele in $Chk2^{-/-}$ cells, indicating that initiation of IR-induced G1/S arrest is independently regulated by Chk1 and Chk2.

Given that initiation of the G1/S checkpoint is regulated by p53 and Cdc25A (Bartek and Lukas, 2001), we examined changes in the expression of p53 and Cdc25A after IR. The level of p53 was increased as early as 1 h and then decreased at 2 h after IR in $Chk1^{+/+}Chk2^{+/+}$ and $Chk1^{+/+}Chk2^{+/-}$ cells (Figure 2B). This increase in p53 protein level was reduced in $Chk1^{+/+}Chk2^{-/-}$ and $Chk1^{+/-}Chk2^{+/-}$ cells and was not observed at all in $Chk1^{+/-}Chk2^{-/-}$ cells. Surprisingly, the level of p53 was significantly higher in the absence of DNA damage in $Chk1^{+/-}Chk2^{+/-}$ and $Chk1^{+/-}Chk2^{-/-}$ cells. Consistent with these effects on p53 level, induction of p21 expression was not detectable in $Chk1^{+/+}Chk2^{-/-}$ or $Chk1^{+/-}Chk2^{-/-}$ cells. In contrast to p53, the level of Cdc25A was very low in the absence of DNA damage in $Chk2^{-/-}$ cells and the abrupt reduction of Cdc25A after DNA damage was significantly impaired by the single deletion of one *Chk1* allele. These results suggest that Chk1 and Chk2 cooperatively regulate the initiation of the G1/S checkpoint through regulation of Cdc25A protein level. Our results also show that Chk2 is required to maintain a proper level of Cdc25A in the absence of DNA damage, but not after DNA damage, although the molecular mechanism remains to be clarified.

P53 protein level is regulated at multiple levels, transcriptionally, translationally and post-translationally (Appella and Anderson, 2001). One of these controls is Chk1- and Chk2-dependent phosphorylation of p53 at S23 in mice (corresponding to S20 in human) (Shieh *et al*, 2000) and subsequent p53 stabilization by prevention of its interaction with the ubiquitin ligase Mdm2 (Chehab *et al*, 1999). The level of p53 phosphorylation at S23 was increased as early as 1 h and then decreased at 4 h after IR in $Chk1^{+/+}Chk2^{+/+}$ and $Chk1^{+/+}Chk2^{+/-}$ cells, whereas the increase was slightly less in $Chk1^{+/+}Chk2^{-/-}$ and $Chk1^{+/-}Chk2^{+/+}$ cells and was only a little in $Chk1^{+/-}Chk2^{+/-}$ and $Chk1^{+/-}Chk2^{-/-}$ cells (Figure 2C). These results suggest that Chk1 and Chk2 independently phosphorylate p53 at S23 after DNA damage and cooperatively regulate its stability.

With respect to the intra-S phase checkpoints, we found that IR reduced incorporation of radio-labelled thymidine to 39% in $Chk1^{+/+}Chk2^{+/+}$ cells as compared with untreated cells (Figure 2D). This reduction was significantly impaired in $Chk1^{+/+}Chk2^{-/-}$ cells (51%, $P<0.05$), $Chk1^{+/-}Chk2^{+/+}$ cells (49%, $P<0.05$) and $Chk1^{+/-}Chk2^{-/-}$ cells (65%, $P<0.01$). Therefore, these results show that the intra-S phase checkpoint in response to double-stranded breaks (DSBs) was regulated by both Chk1 and Chk2.

We next examined IR-induced G2 checkpoint function. In contrast to the G1 checkpoint, loss of a single *Chk1* allele resulted in an impaired IR-induced G2 arrest at both low

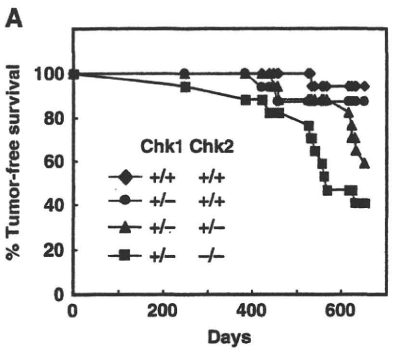

B

Genotypes	Sex/age (week)	Histology
$Chk1^{+/-}Chk2^{-/-}$	M/36	Malignant lymphoma
	F/54	Malignant lymphoma
	M/62	Malignant lymphoma, lung adenoma
	F/73	Malignant lymphoma
	F/75	Malignant lymphoma
	M/75	Malignant lymphoma
	F/77	Malignant lymphoma
	F/79	Subcutaneous sarcoma
	M/81	Malignant lymphoma, lung adenoma
	F/89	Malignant lymphoma
$Chk1^{+/-}Chk2^{+/-}$	M/63	Pancreas adenocarcinoma
	F/65	Malignant lymphoma
	F/88	Malignant lymphoma
	F/88	Lower abdominal sarcoma
	M/89	Lung adenocarcinoma
	F/90	Malignant lymphoma
	F/93	Malignant lymphoma

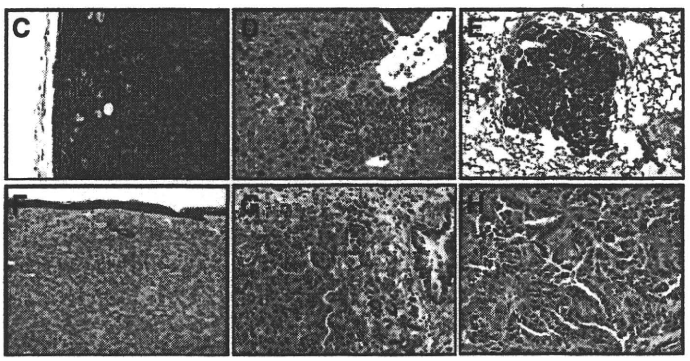

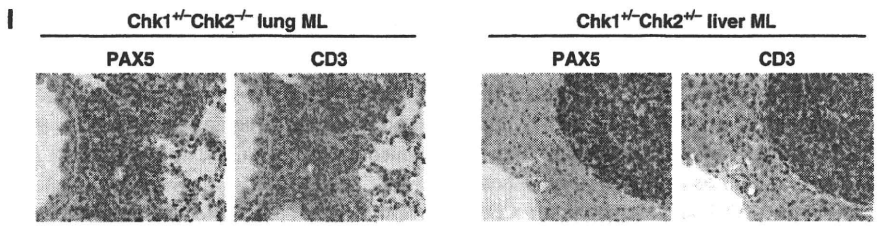

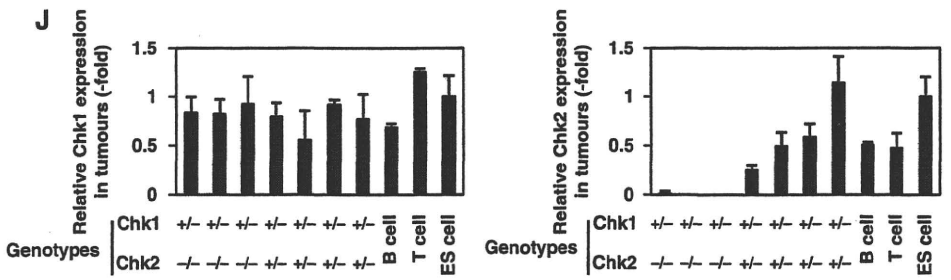

Figure 1 Development of spontaneous tumours in mice bearing germline deletions of *Chk1* and *Chk2*. (**A**) Kaplan–Meier analysis of tumour-free survival of wild type (diamonds, $n=17$), $Chk1^{+/-}Chk2^{+/+}$ (circles, $n=15$), $Chk1^{+/-}Chk2^{+/-}$ (triangles, $n=17$) and $Chk1^{+/-}Chk2^{-/-}$ (squares, $n=17$) mice. The animals were monitored for up to 22 months or until they succumbed to cancer. All tumour cases were identified based on the results of pathological analysis. The statistical significance of the survival curves was assessed using the log-rank test. (**B**) Table summarizing the cancer types observed in $Chk1^{+/-}Chk2^{-/-}$ and $Chk1^{+/-}Chk2^{+/-}$ mice, together with the sexes and ages of the mice; 59% of $Chk1^{+/-}Chk2^{-/-}$, 41% of $Chk1^{+/-}Chk2^{+/-}$, 13% of $Chk1^{+/-}Chk2^{+/+}$ and 6% of $Chk1^{+/+}Chk2^{+/+}$ mice succumbed to cancer during this experimental period. (**C–H**) Images of haematoxylin and eosin histology of six representative tumours found in $Chk1^{+/-}Chk2^{+/-}$ and $Chk1^{+/-}Chk2^{-/-}$ mice. A malignant lymphoma in a lymph node of a $Chk1^{+/-}Chk2^{-/-}$ mouse, ×200 (**C**); a malignant lymphoma in the liver of a $Chk1^{+/-}Chk2^{-/-}$ mouse, ×200 (**D**); a lung adenoma in a $Chk1^{+/-}Chk2^{-/-}$ mouse, ×100 (**E**); a subcutaneous sarcoma in $Chk1^{+/-}Chk2^{-/-}$ mice, ×100 (**F**); a pancreatic adenocarcinoma, ×200 (**G**) and a lung adenocarcinoma, ×200 (**H**). (**I**) Representative immunohistochemical staining of a malignant lymphoma invading the lung of a $Chk1^{+/-}Chk2^{-/-}$ mouse (left) and liver of a $Chk1^{+/-}Chk2^{+/-}$ mouse (right) with PAX5 used as a B-cell marker and CD3 as a T-cell marker, ×100. PAX5 was positive in the nucleus of invading atypical small round cells and CD3 was negative in the membrane of these cells. (**J**) Expression of Chk1 (left panel) and Chk2 (right panel) transcripts in tumours from $Chk1^{+/-}Chk2^{+/-}$ and $Chk1^{+/-}Chk2^{-/-}$ mice. Expression levels of Chk1 and Chk2 transcripts were measured by real-time PCR using RNAs prepared from paraffin-embedded tumour tissues and RNAs from B cells, T cells and ES cells as controls. Normalization was performed relative to the level of GAPDH transcripts and the data are presented as relative expressions to those in ES cells.

(1 Gy) and high (3 Gy) doses of irradiation (Figure 2E), whereas null depletion of *Chk2* had no effect in this regard. Consistent with our observations, recent reports have shown that Chk2 is dispensable for the degradation of Cdc25A and initiation of G2/M arrest after DNA damage in human (Jallepalli *et al*, 2003; Jin *et al*, 2008), mouse (Takai *et al*,

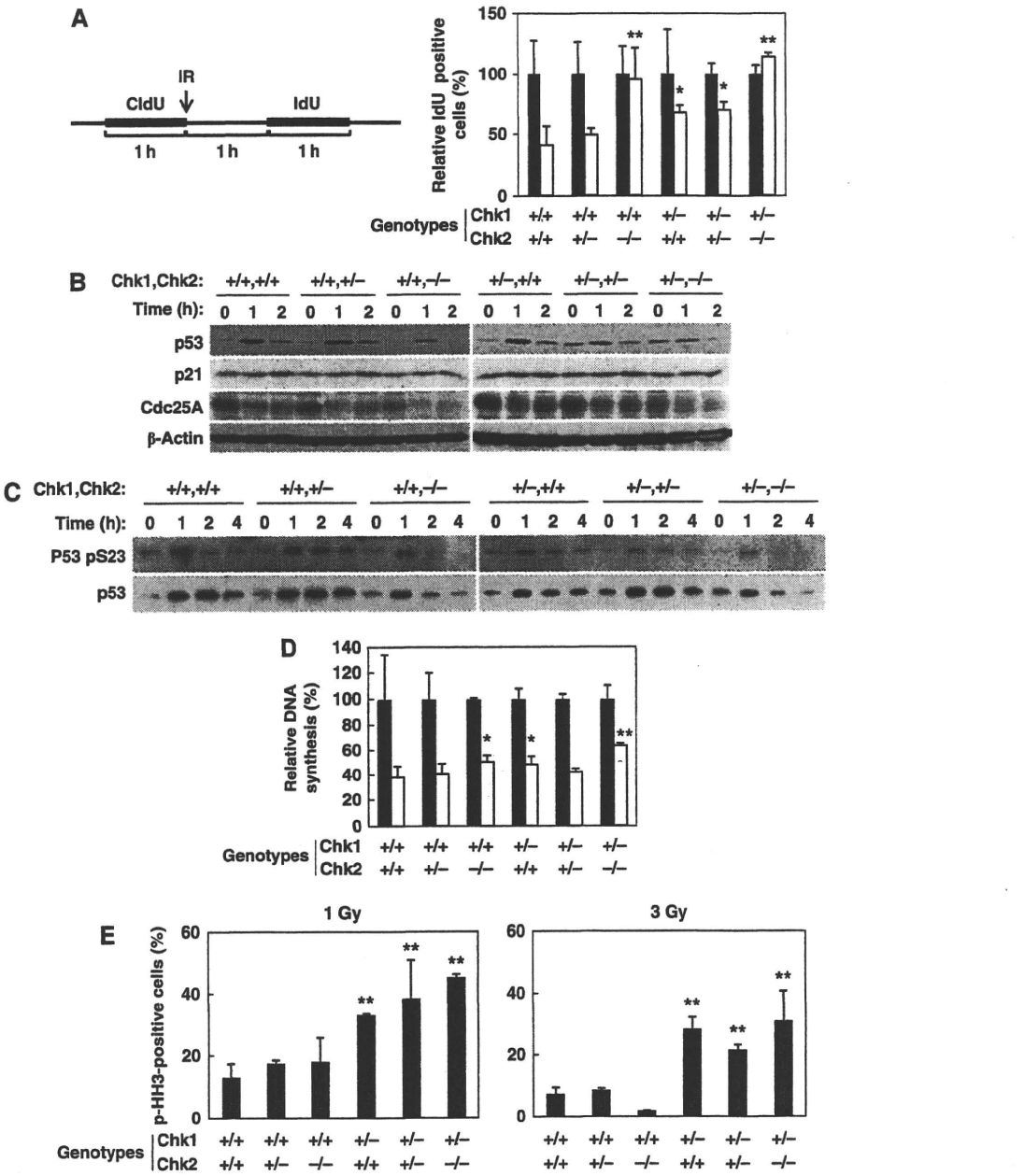

Figure 2 Chk1 and Chk2 regulate non-redundant DNA-damage checkpoints. (**A**) Synergistic regulation of G1/S checkpoint by Chk1 and Chk2. Diagram of our strategy to assess the G1/S checkpoint after IR irradiation. Primary MEFs with the indicated genotypes are labelled with CIdU for 1 h and then IR irradiated (white bars) or mock irradiated (black bars). After washing out the CIdU, the cells were incubated in fresh medium for 1 h and then incubated with IdU for 1 h. In order to record the number of cells newly entering S phase after IR irradiation, single IdU-positive cells were counted (at least 300 cells) and the results were represented as a percentage of the total cells. Data are means ± s.d. of at least three independent experiments. Statistical significance compared with $Chk1^{+/+}Chk2^{+/+}$ MEFs was assessed by Student's *t*-test (*$P<0.05$, **$P<0.01$). (**B**) Accumulation of p53 and reduction of Cdc25A upon IR treatment. Primary MEFs with the indicated genotypes were irradiated with IR (4 Gy) and harvested at 0, 1 and 2 h after irradiation. Cell lysates were subjected to immunoblotting using anti-p53 (upper panels), anti-p21 (2nd panels), anti-Cdc25A (3rd panels) and anti-β-actin (bottom panels) antibodies. (**C**) Phosphorylation of p53 at S23 after IR treatment. Primary MEFs with the indicated genotypes were irradiated with IR (4 Gy) and harvested at 0, 1, 2 and 4 h after irradiation. Cell lysates were immunoprecipiated with anti-p53 antibodies and the precipitates were subjected to immunoblotting using an anti-phospho-p53 at S23 antibody (upper panels) and an anti-p53 antibody (lower panels). (**D**) Radio-resistant DNA synthesis was examined as described in Materials and methods. The rate of DNA synthesis was determined by the radioactivity of [^{3}H] divided by that of [^{14}C]. The relative DNA synthesis is represented as a percentage of DNA synthesis relative to that observed in cells without DNA damage. Data are means ± s.d. of at least three independent experiments. Statistical significance compared with $Chk1^{+/+}Chk2^{+/+}$ MEFs was assessed by Student's *t*-test (*$P<0.05$, **$P<0.01$). (**E**) Defective G2/M checkpoint in mice lacking a single Chk1 allele. Primary MEFs from mice with the indicated genotypes were treated with two distinct doses of IR (1 Gy: left panel and 3 Gy: right panel). The mitotic index was determined as the percentage of mitotic cells (pH3 Ser10 positive) relative to the total cells at 0.5 h after irradiation. The mitotic index was then calculated as a percentage relative to the non-irradiated cells. Data are means ± s.d. of at least three independent experiments. Statistical significance compared with $Chk1^{+/+}Chk2^{+/+}$ MEFs was assessed by Student's *t*-test (**$P<0.01$).

2002) and Drosophila cells (Varmark *et al*, 2010). Thus, our results suggest that IR-induced G2 arrest is mainly regulated by Chk1, although maintenance of G2 arrest might be affected by Chk2 depletion as reported earlier (Hirao *et al*, 2000; Yu *et al*, 2001).

Aberrant DNA-damage-induced apoptosis and DNA-repair activity in Chk1/Chk2 double-mutant cells

Chk2 has been reported to regulate DNA-damage-induced apoptosis (Hirao *et al*, 2002; Takai *et al*, 2002). Therefore, it is possible that Chk1 and Chk2 may cooperatively regulate p53-dependent apoptosis. Thymocytes from Chk-depleted mice were irradiated and their survival was assessed. Depletion of two *Chk2* alleles, but not a single *Chk1* allele, resulted in impaired induction of thymocyte apoptosis after IR treatment at a high dose (4 Gy) (Figure 3A, right panel). Intriguingly, deletion of a single Chk2 allele also resulted in a partial impairment of apoptosis at a low dose (1 Gy) of IR (Figure 3A, left panel), suggesting that Chk2 is haplo-insufficient for induction of apoptosis.

We then sought to determine whether impaired induction of apoptosis in Chk2-depleted thymocytes was due to reduced induction of p53 protein upon DNA damage. Induction of p53 was observed as early as 1 h and peaked at 2 h after IR in $Chk1^{+/+}Chk2^{+/+}$ thymocytes (Figure 3B). This induction was severely impaired in $Chk1^{+/+}Chk2^{-/-}$ and $Chk1^{+/-}Chk2^{-/-}$ thymocytes. It should be noted that, unlike MEFs, thymocytes from $Chk1^{+/-}Chk2^{+/-}$ and $Chk1^{+/-}Chk2^{-/-}$ mice did not contain a higher level of p53 under unperturbed conditions when compared with $Chk1^{+/+}Chk2^{+/+}$ mice. These results suggest that Chk2 regulates IR-induced apoptosis in thymocytes at least in part through induction of p53 expression.

Chk1 and Chk2 are reported to be involved in DNA repair through phosphorylation of Rad51 (Sorensen *et al*, 2005) and BRCA1 (Lee *et al*, 2000), respectively. Therefore, the cooperative effect of Chk1 and Chk2 in suppressing tumourigenesis may be explained by their ability to ensure proper DNA repair. To address this question, we analysed DNA repair in double Chk1- and Chk2-depleted primary MEFs using an

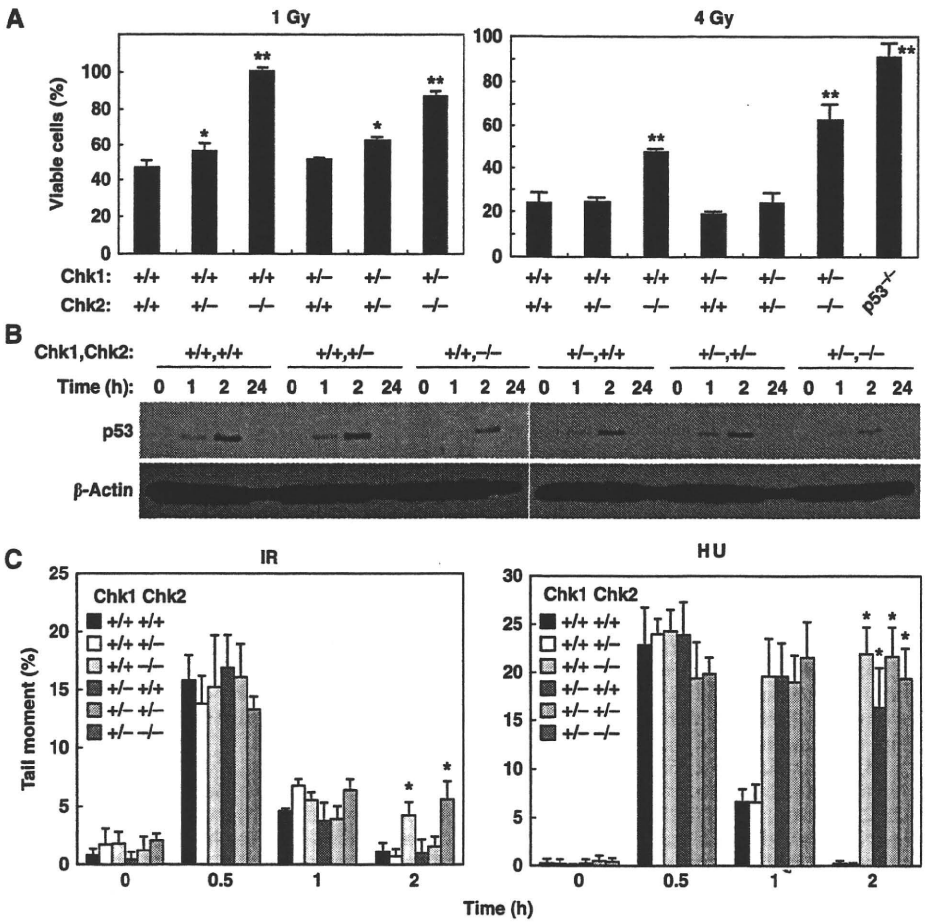

Figure 3 Chk1 and Chk2 have a non-redundant function in DNA-damage-induced apoptosis and DNA repair. (**A**) Chk2 is haplo-insufficient for IR-induced apoptosis of thymocytes. Thymocytes from mice with the indicated genotypes were exposed to 1 Gy (left panel) or 4 Gy (right panel) irradiation. Sub G1 population was determined by FACS and viable cells were calculated as a percentage of non-sub G1 cells relative to the total cell number. Data are means ± s.d. of at least three independent experiments. Statistical significance compared with $Chk1^{+/+}Chk2^{+/+}$ MEFs was assessed by Student's *t*-test (*$P<0.05$, **$P<0.01$) (**B**) Accumulation of p53 upon IR treatment in thymocytes. Thymocytes from mice with the indicated genotypes were irradiated with IR (4 Gy) and harvested at 0, 1, 2 and 24 h after irradiation. Cells were subjected to immunoblotting using anti-p53 and anti-β-actin antibodies. (**C**) Chk1 and Chk2 regulate the efficiency of DNA repair. Primary MEFs of the indicated genotypes were treated with IR (left panel) or hydroxyurea (HU: right panel) and subjected to an alkaline-comet assay at the indicated times. Tail moments were determined using TriTek Comet Score Freeware. Data are means ± s.d. of counting at least 50 cells per sample in three independent experiments. Statistical significance compared with $Chk1^{+/+}Chk2^{+/+}$ MEFs was assessed by Student's *t*-test (*$P<0.005$).

alkaline-comet assay. Deletion of two *Chk2* alleles resulted in a significant aberration of IR-induced DNA repair, although loss of a single *Chk1* allele had no effect (Figure 3C). In contrast, loss of a single *Chk1* allele, as well as deletion of two *Chk2* alleles, caused aberrant DNA repair when DNA damage was induced by hydroxyurea. This indicated that DNA damage-induced activation of DNA repair requires Chk1 or Chk2, but which is required depends on the type of DNA damage.

Spontaneous DNA damage in proliferating Chk1$^{+/-}$ Chk2$^{+/-}$ and Chk1$^{+/-}$Chk2$^{-/-}$ MEFs under unperturbed condition

The increase in the level of p53 observed in proliferative *Chk1*$^{+/-}$*Chk2*$^{+/-}$ and *Chk1*$^{+/-}$*Chk2*$^{-/-}$ MEFs under unperturbed conditions (Figure 2B) raises the possibility that Chk1 and Chk2 directly regulate factors that determine p53 stabilization or prevent accumulation of spontaneous DNA damage that eventually increases p53 protein levels. In *Chk1*$^{+/+}$*Chk2*$^{+/+}$ MEFs, IR induced a biphasic increase in p53, showing a rapid induction of expression within 4 h and a slow induction at 24 h (Figures 2B and 4A). A similar IR-induced biphasic accumulation of p53 was also reported in normal human embryonic cells (Ghosh *et al*, 2000). As seen in Figure 2B, an increased level of p53 was detected in *Chk1*$^{+/-}$*Chk2*$^{+/-}$ and *Chk1*$^{+/-}$*Chk2*$^{-/-}$ MEFs under unperturbed conditions (time 0). The level of p21 was also higher in these cells under unperturbed conditions. Surprisingly, the level of Mdm2 was very low in *Chk1*$^{+/-}$*Chk2*$^{-/-}$ MEFs, although the level of p53, a transcriptional activator of Mdm2, was high during this experimental period, suggesting that Chk1 and Chk2 may cooperatively stabilize Mdm2 through an unknown mechanism. In contrast to apparent impairment of the rapid accumulation of p53 observed in *Chk1*$^{+/-}$*Chk2*$^{+/-}$ and *Chk1*$^{+/-}$*Chk2*$^{-/-}$ MEFs, a slow induction was observed in all other MEFs tested. Recently, it was reported that Che-1, an RNA polymerase II-binding protein, was phosphorylated by ATM/ATR and Chk1 after DNA damage (Bruno *et al*, 2006). The phosphorylation of Che-1 resulted in its accumulation and recruitment to the *p53* promoter to activate *p53* gene transcription. We examined the induction of Che-1 as well as changes in p53 transcript level after DNA damage. However, in contrast to the previous report (Bruno *et al*, 2006), the accumulation of Che-1 was only impaired upon Chk2 deletion (*Chk1*$^{+/+}$*Chk2*$^{-/-}$ and *Chk1*$^{+/-}$*Chk2*$^{-/-}$ MEFs) when compared with what is observed in *Chk1*$^{+/+}$*Chk2*$^{+/+}$ MEFs (Figure 4A). Deletion of a single *Chk1* allele did appear to slightly affect accumulation of Che-1, consistent with the previous observation that Chk1 as well as Chk2 could phosphorylate Che-1 *in vitro*. P53 transcription was increased as early as 4 h after DNA damage and then decreased in *Chk1*$^{+/+}$*Chk2*$^{+/+}$ and *Chk1*$^{+/-}$*Chk2*$^{+/+}$ MEFs, whereas it did not vary in MEFs in which either 1 or 2 copies of *Chk2* were deleted (Figure 4B). These results show that a single *Chk2* allele is not sufficient for recruitment of Che-1 to the p53 promoter and, therefore, Chk2 is haplo-insufficient for Che-1-dependent transcriptional activation of p53. However, this transcriptional activation was apparently not involved in the slow induction of p53 expression after DNA damage.

Given that a significant number of heterozygous lobuloalveolar mammary epithelial cells contained spontaneous DNA damage in *Chk1* conditional heterozygotes (Lam *et al*, 2004), we speculate that this was also the case in primary MEFs from *Chk1* heterozygotes. To examine this possibility, MEFs from *Chk1/Chk2* double-mutant mice were stained with phospho-H2AX specific for Ser139 (γH2AX) without the addition of any exogenous DNA-damaging agent. A significant number of γH2AX-positive cells were readily detected in *Chk1*$^{+/-}$*Chk2*$^{+/-}$ and *Chk1*$^{+/-}$*Chk2*$^{-/-}$ MEFs, but not in MEFs from other genotypes (Figure 4C). Signals for γH2AX in *Chk1*$^{+/-}$*Chk2*$^{-/-}$ MEFs were much stronger than those in *Chk1*$^{+/-}$*Chk2*$^{+/-}$ MEFs. However, some of the γH2AX signals in *Chk1*$^{+/-}$*Chk2*$^{-/-}$ MEFs as well as most of the signals in *Chk1*$^{+/-}$*Chk2*$^{+/-}$ MEFs showed typical discrete foci, presumably because of the level of spontaneous DNA damage. These results suggest that Chk1 and Chk2 cooperatively prevent the accumulation of cells with spontaneous DNA damage.

Accumulation of DNA damage can easily result in genome instability. We thus examined metaphase chromosome spreads from *Chk1/Chk2* double-mutated primary MEFs and CD19-positive B cells. Aberrations including chromosomal breaks and many fusions appeared in *Chk1*$^{+/-}$*Chk2*$^{+/-}$ and *Chk1*$^{+/-}$*Chk2*$^{-/-}$ MEFs (Table I). Although the level of the chromosomal aberrations observed in the activated B cells was relatively low when compared with MEFs, presumably because of the short *in vitro* culture period (72 h) of B cells, higher levels of chromosomal aberrations were detected in B cells from *Chk1*$^{+/-}$*Chk2*$^{+/-}$ and *Chk1*$^{+/-}$*Chk2*$^{-/-}$ mice (Table II). These results confirm that *Chk1*$^{+/-}$*Chk2*$^{+/-}$ and *Chk1*$^{+/-}$*Chk2*$^{-/-}$ mice are more susceptible to B-cell lymphomas and show that Chk1 and Chk2 synergistically prevent susceptibility to global chromosomal rearrangement.

Chk1 and Chk2 do not appear to be involved in the induction of premature senescence

Senescence offers a major protective mechanism against tumour development and is triggered by DNA damage responses (Lowe *et al*, 2004). In several studies using human diploid cells, activation of Chk1 and Chk2 was proposed to be important for oncogene-induced and replicative senescence (d'Adda di Fagagna *et al*, 2003; Bartkova *et al*, 2006; Di Micco *et al*, 2006; Mallette *et al*, 2007). Therefore, we hypothesized that the cooperative function of Chk1 and Chk2 in suppression of tumourigenesis might be a means to ensure induction of senescence upon exposure of cells to genotoxic stress. To test this hypothesis, we first examined stress-induced senescence in culture, known as 'culture shock', in which mammalian cells are exposed to an unrelenting onslaught of mitogenic signals (Sherr and DePinho, 2000). Wild type and other types of Chk1/Chk2-depleted primary MEFs tested were cultured in serum-containing medium and passaged every 3 days after a 3T3 subculture schedule. All types of MEFs had similar doubling times for the first 10 generations. Their growth rate then slowed and eventually reached a non-dividing state even at a subconfluent density (Figure 5A). These cells then recovered their growth capability and became immortal at around 40 days with a doubling time similar to that of the initial culture. Unexpectedly, ectopic expression of oncogenic Ras clearly induced both growth arrest (Figure 5B) and a senescent phenotype as assessed by senescence-associated β-gal staining (Figure 5C) in all types of double Chk1- and Chk2-depleted primary MEFs.

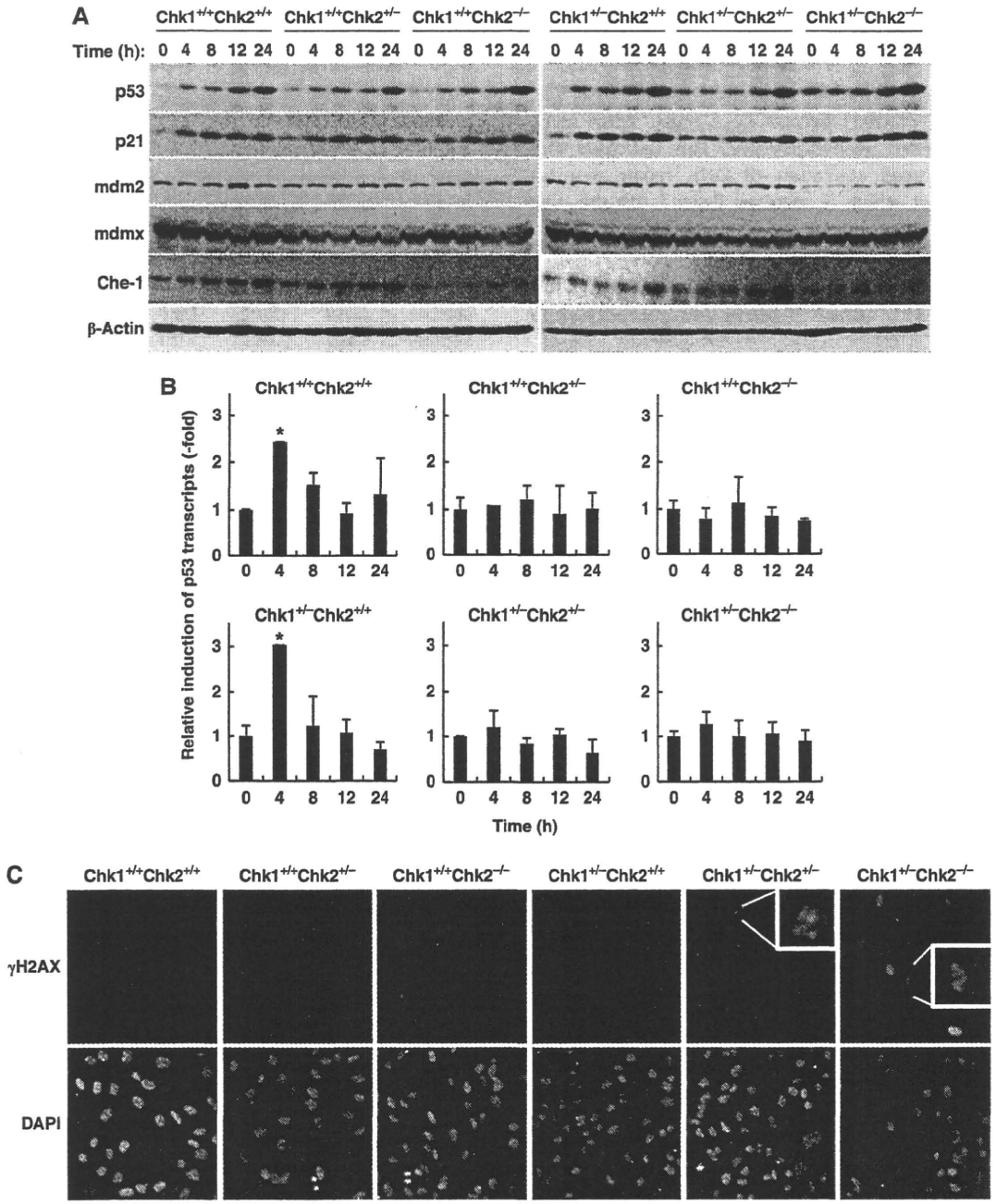

Figure 4 Spontaneous DNA damage and induction of p53 under unperturbed conditions in *Chk1*$^{+/-}$*Chk2*$^{+/-}$ and *Chk1*$^{+/-}$*Chk2*$^{-/-}$ MEFs. (**A**) Cell lysates from the indicated MEFs were irradiated with IR (4 Gy). Cells were harvested at the indicated times after IR and cell lysates were subjected to immunoblotting with anti-p53 (top), anti-p21 (second), anti-mdm2 (third), anti-mdmX (fourth), anti-Che-1 (fifth) and anti-β-actin (bottom) antibodies. (**B**) Changes in the p53 transcripts after IR irradiation. Primary MEFs with the indicated genotypes were irradiated with IR (4 Gy) and harvested at the indicated times after irradiation. Total RNA was then extracted and the expression levels of p53 transcript were measured by quantitative real-time PCR. The results were normalized to the level of GAPDH transcripts used as an internal control and data are presented as means ± s.d. of at least three independent experiments. Statistical significance compared with cells without IR irradiation (time 0) was assessed by Student's *t*-test (*$P<0.01$). (**C**) Spontaneous DNA damage under unperturbed conditions in *Chk1*$^{+/-}$*Chk2*$^{+/-}$ and *Chk1*$^{+/-}$*Chk2*$^{-/-}$ MEFs. Asynchronized primary MEFs with the indicated genotypes without any genotoxic stress were fixed and subjected to immunofluorescence staining with anti-phospho-H2AX (γH2AX) antibodies (upper panel). Cells were counterstained with DAPI to detect nuclei (lower panel), × 200. Magnified images of cells with γH2AX foci are shown in the white boxes (*Chk1*$^{+/-}$*CHk2*$^{+/-}$ and *Chk1*$^{+/-}$*Chk2*$^{-/-}$ cells).

Given that homozygous deletion of *Chk1* resulted in growth arrest at S phase (Shimada and Nakanishi, 2008) and presented a senescence-like morphology, and knockdown of Chk1 by its siRNA drastically increased the number of SA-β-gal-positive cells (Shimada *et al*, paper in preparation), our results indicated that both Chk1 and Chk2 are apparently dispensable for oncogene-induced senescence.

As the induction of senescent phenotypes is regulated by both p16-Rb and p53-dependent mechanisms (Courtois-Cox

Table I Chromosomal abnormalities in primary MEFs from Chk1/Chk2 double-mutant mice[a]

Samples	Metaphases analysed	Chromosomes/metaphase	Total aberrant cells (%)
$Chk1^{+/+}Chk2^{+/+}$	58	40.30 ± 0.60	2 (3.45%)
$Chk1^{+/+}Chk2^{+/-}$	62	40.37 ± 1.09	4 (6.45%)
$Chk1^{+/+}Chk2^{-/-}$	58	42.54 ± 1.38	9 (15.52%)
$Chk1^{+/-}Chk2^{+/+}$	59	39.96 ± 0.66	5 (8.47%)
$Chk1^{+/-}Chk2^{+/-}$	58	40.66 ± 0.61	11 (18.97%)
$Chk1^{+/-}Chk2^{-/-}$	59	44.12 ± 1.56	12 (20.34%)

[a]Chromosomes were stained with 4', 6'-diamidino-2-phenylindole (DAPI) and observed under a Zeiss axioplan imaging 2 microscope. The abnormal chromosomes including fusions and fragments were counted in metaphase chromosome spreads of MEFs with the indicated genotypes.

Table II Chromosomal abnormalities in primary B cells from Chk1/Chk2 double-mutant mice[a]

Samples	Metaphases analysed	Chromosomes/metaphase	Total aberrant cells (%)
$Chk1^{+/+}Chk2^{+/+}$	65	39.97 ± 0.17	1 (1.54%)
$Chk1^{+/+}Chk2^{+/-}$	52	39.88 ± 0.61	1 (1.92%)
$Chk1^{+/+}Chk2^{-/-}$	55	39.53 ± 1.36	3 (5.45%)
$Chk1^{+/-}Chk2^{+/+}$	36	37.80 ± 3.38	2 (5.56%)
$Chk1^{+/-}Chk2^{+/-}$	37	39.02 ± 2.11	3 (8.11%)
$Chk1^{+/-}Chk2^{-/-}$	33	39.39 ± 1.03	3 (9.09%)

[a]Primary B cells from *Chk1/Chk2* double-mutant mice were isolated using magnetic bead-conjugated antibodies against CD19 and AutoMACS, and stimulated by lipopolysaccharide as described in 'Materials and methods'. Chromosomes were stained with 4', 6'-diamidino-2-phenylindole (DAPI) and observed under a Zeiss axioplan imaging 2 microscope. The abnormal chromosomes including fusions and fragments were counted in metaphase chromosome spreads of B cells with the indicated genotypes.

et al, 2008), we wondered whether senescent phenotypes in Chk-depleted MEFs were induced by either or both pathways. Expression of oncogenic Ras resulted in the clear induction of p16 protein in all types of MEFs (Figure 5D). As described above, the level of p53 was significantly higher in control-transfected $Chk1^{+/-}Chk2^{+/-}$ and $Chk1^{+/-}Chk2^{-/-}$ MEFs than in MEFs of other genotypes. Intriguingly, the levels of p53 and p21 in control-transfected $Chk1^{+/-}Chk2^{-/-}$ MEFs were almost identical to those observed in Ras-transfected senescent cells. These results suggest that senescent phenotypes among $Chk1^{+/-}Chk2^{-/-}$ MEFs might be induced by activation of p16-Rb pathway. To further clarify this point, we introduced papillomavirus E7, which binds to and inactivates Rb (Chellappan *et al*, 1992), into $Chk1^{+/-}Chk2^{+/-}$ and $Chk1^{+/-}Chk2^{-/-}$ primary MEFs in the presence or absence of oncogenic Ras. Surprisingly, E7 failed to prevent growth arrest and a senescence-like cell morphology in $Chk1^{+/-}Chk2^{+/-}$ and $Chk1^{+/-}Chk2^{-/-}$ primary MEFs expressing oncogenic Ras as well as in $Chk1^{+/+}Chk2^{+/+}$ MEFs cells (Figure 6A and B). Co-introduction of papillomavirus E6, which targets p53 for degradation (Scheffner *et al*, 1990), with E7 completely reversed growth arrest and morphological changes in $Chk1^{+/-}Chk2^{+/-}$ and $Chk1^{+/-}Chk2^{-/-}$ primary MEFs expressing oncogenic Ras. These results indicate that senescence is induced in $Chk1^{+/-}Chk2^{+/-}$ and $Chk1^{+/-}Chk2^{-/-}$ cells at least in part by oncogene-induced activation of the p53 pathway even in the absence of p16-Rb pathway. Although the actual contribution of the p16-Rb pathway to senescence induction in $Chk1^{+/-}Chk2^{+/-}$ and $Chk1^{+/-}Chk2^{-/-}$ MEFs is unknown, it should be noted that abrogation of a p53-Arf pathway (Serrano *et al*, 1997; Palmero *et al*, 1998), but not loss of p16 (Sharpless *et al*, 2001), is sufficient to prevent oncogenic Ras-induced senescence in primary MEFs. Taken together, our results indicate that cancer predisposition of $Chk1^{+/-}Chk2^{+/-}$ and $Chk1^{+/-}Chk2^{-/-}$ mice is not due to impaired induction of senescence in response to genotoxic stress.

Discussion

Our results clearly indicate that Chk1 and Chk2 act cooperatively to prevent tumourigenesis by regulating partly redundant, but mainly non-redundant responses to DNA damage or genotoxic stress, including cell cycle arrest, apoptosis and DNA repair. As a result, combined loss of Chk1 and Chk2 causes the accumulation of cells with spontaneous DNA damage under unperturbed conditions leading to genomic instability and then tumour development. Accumulation of cells with DNA damage under unperturbed conditions appears to result from increased DNA damage during S phase because of reduced Chk1 activity and failure to eliminate cells with DNA damage by loss of Chk2 function. This idea is strongly supported by the fact that Chk1 depletion causes severe DNA damage during S phase (Niida *et al*, 2005; Syljuasen *et al*, 2005) and that Chk2-deficient MEFs are highly resistant to DNA-damage-induced apoptosis (Figure 3A) (Hirao *et al*, 2002; Takai *et al*, 2002). In addition, increased expression of p53 in Chk1/Chk2 double-depleted cells under unperturbed conditions was observed only in proliferative MEFs and not in G0-arrested T cells (Figures 2B, 3B and 4A), further supporting the idea that DNA damage in these cells occurred during S phase. Recently, Zaugg *et al* (2007) reported that Chk1 and Chk2 functioned in mostly non-redundant DNA-damage response and that the loss of Chk1 activated Chk2 in thymocytes, suggesting the existence of physiological cross-talk between Chk1 and Chk2. Taken together, these results indicate that high tumour susceptibility

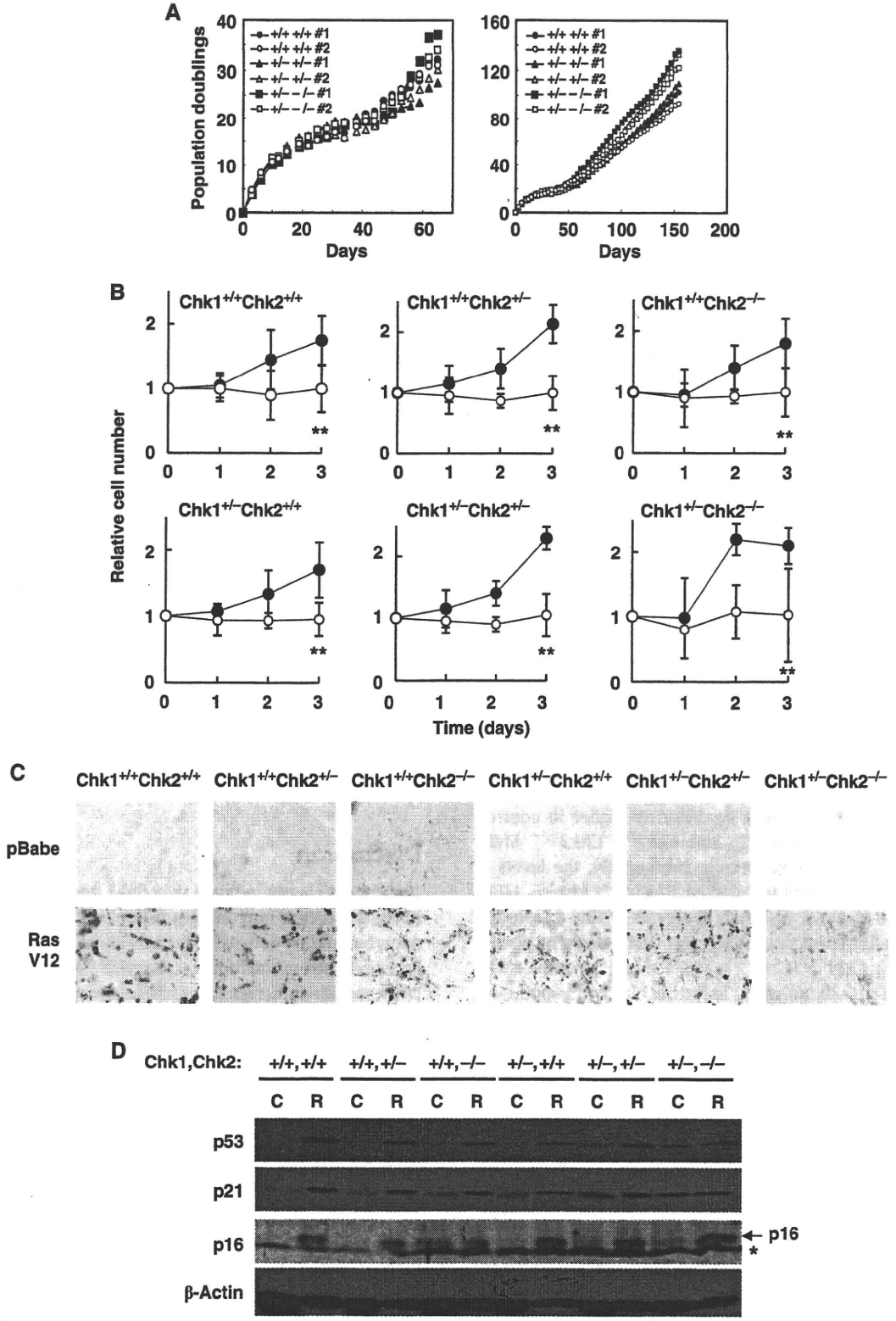

Figure 5 Chk1 and Chk2 are apparently dispensable for culture-induced (culture shock) and oncogene-induced senescence. (**A**) Growth rates of short-term (left panel) and long-term (right panel) cultures of primary MEFs of the indicated genotypes. (**B**) Representative growth curves corresponding to primary MEFs with the indicated genotypes infected with control (closed circles) or H-RasV12-expressing (open circles) retroviruses. Statistical significance of relative numbers of cells expressing RasV12 at day 3 compared with those expressing control vector was assessed by Student's *t*-test (**$P<0.01$). (**C**) Photographs of cells stained for SA-β-gal activity 3 days after infection. (**D**) Induction of p53, p21 and p16 proteins in cells of the indicated genotypes infected with either control (C) or H-RasV12 (R). An asterisk represents non-specific bands.

in *Chk1*$^{+/-}$*Chk2*$^{+/-}$ and *Chk1*$^{+/-}$*Chk2*$^{-/-}$ mice is likely due to the combined impairment of non-redundant DNA-damage response mediated by both Chk1 and Chk2.

Although mutations in *CHEK2* (the gene encoding Chk2) do not account for the cancer-predisposing Li–Fraumeni syndrome as originally thought, rare germline mutations

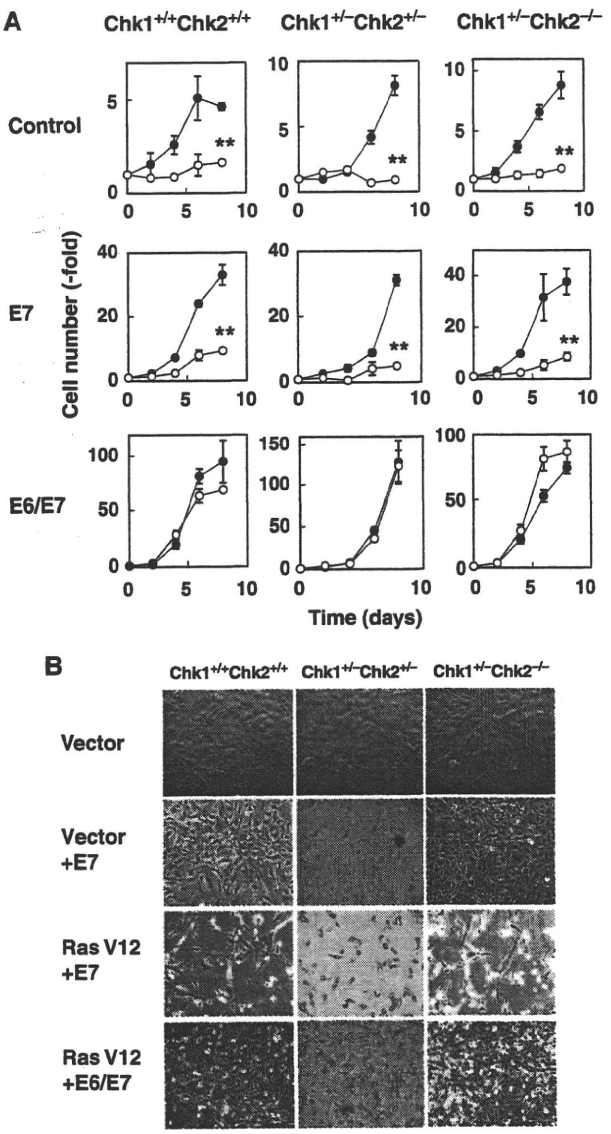

Figure 6 Chk1 and Chk2 are apparently dispensable for p53- and Rb-dependent senescence pathways. (**A**) Growth curve of MEFs with or without RasV12-expressing mock (control), E7 (E7) or both E6 and E7 (E6/E7). The cells were infected with empty (open circles) or Ras-expressing retrovirus (filled circles). Cell numbers were counted at the indicated times after selection. Data are means ± s.d. of triplicate experiments. Statistical significance of relative numbers of cells expressing RasV12 at day 8 compared with those expressing control vector was assessed by Student's *t*-test (**$P<0.01$). (**B**) Morphology of cells obtained at 8 days after selection. The MEFs expressing mock (top panel), E7 (second and third panels) and E6/E7 (bottom panel) were infected with empty (top and second panels) or Ras-expressing retrovirus (third and bottom panels).

have been detected with high incidence in a number of familial cancers and rare somatic mutations have been reported in some tumours, suggesting that *CHEK2* is indeed a cancer susceptibility gene (Meijers-Heijboer *et al*, 2002; Vahteristo *et al*, 2002; Antoni *et al*, 2007). However, we and others have shown that complete loss of both Chk2 alleles is not sufficient to increase tumour incidence in mice (Hirao *et al*, 2002; Takai *et al*, 2002). In this regard, it should be noted that most of the *CHEK2* abnormalities in human tumours are mutations (not complete gene deletion) that generate truncated or mutated forms of the Chk2 protein (Antoni *et al*, 2007). Thus, these modified forms may impair other tumour suppressive pathways in a dominant-negative manner. Alternatively, it may take a much longer time to generate tumours by loss of Chk2 function, so that they are not observed during the short life span of the mice.

Chk1$^{+/-}$*Chk2*$^{+/-}$ and *Chk1*$^{+/-}$*Chk2*$^{-/-}$ mice developed B-cell tumours, but not T-cell lymphomas. Intriguingly, B-cell lymphomas have been observed in mice bearing a *p53 S23A/S23A* knockin mutation (corresponding to human S20) (MacPherson *et al*, 2004). It is, therefore, possible that tumourigenicity in the double-mutant mice resulted from impaired phosphorylation of p53 at S23 that is redundantly regulated by both Chk1 and Chk2 in response to DNA damage, as indicated from *in vitro* studies (Shieh *et al*, 2000). P53 is activated by numerous types of stress, such as DNA damage, viral infection and metabolic stress, through phosphorylation of S23. CK1 is a p53 S23 kinase activated in response to DNA viral infection (MacLaine *et al*, 2008), AMPK is another p53 S23 kinase activated in response to elevation of AMP/ATP ratio (Maclaine and Hupp, 2009) and DAPK-1 is a third p53 S23 kinase activated in response to inappropriate oncogene activation (Craig *et al*, 2007). However, the kinase responsible for S23 phosphorylation in response to IR has not been identified. Unexpectedly, knockdown of either or both Chk1 and Chk2 in human cells failed to abrogate the damage-dependent induction of p53 expression (Ahn *et al*, 2003), and depletion of both *Chk2* alleles in human colon cancer cells does not compromise p53 phosphorylation at S20 (corresponding to mouse S23) (Jallepalli *et al*, 2003). Although these results cast doubt on the function of Chk1 and Chk2 in the damage-induced phosphorylation of human p53 at S20 (corresponding to mouse S23), our present results clearly show that DNA-damage-induced mouse p53 phosphorylation at S23 was abrogated in primary MEFs from *Chk1*$^{+/-}$*Chk2*$^{-/-}$ mice. One potential explanation for this discrepancy is that our experiments were performed with primary knockout MEFs, whereas other studies used human cancer cells and did not analyse the phosphorylation status of p53 at S20 (corresponding to mouse S23) in Chk1/Chk2 double-knockdown cells. Therefore, although the contribution of Chk1 and Chk2 to the phosphorylation of p53 at S23 in response to DNA damage appears to be somewhat different between human and mouse cells, both enzymes are likely to function as damage-induced p53 S23 kinases in a redundant manner.

Chk2 has also been reported to cooperate with other factors involved in DNA-damage response to suppress oncogenic potential. For example, *Brca1*$^{\Delta 11/\Delta 11}$*Chk2*$^{-/-}$ mice showed cancer predisposition (Cao *et al*, 2006). Similarly, *Chk2*$^{-/-}$ mice with a conditional deletion of *Brca1* in the thymus or mammary gland developed tumours in these tissues (McPherson *et al*, 2004). Very recently, *NBS1*$^{\Delta B/\Delta B}$ *Chk2*$^{-/-}$ and *Mre11*$^{ATLD1/ATLD1}$*Chk2*$^{-/-}$ mice have also been reported to develop tumours with latency similar to that observed in *Brca1*$^{\Delta 11/\Delta 11}$*Chk2*$^{-/-}$ mice (Stracker *et al*, 2008). Both the MRN complex and Brca1 have an essential function in sensing DNA double-strand breaks and in transmitting the signal to downstream targets. In contrast, Chk1 and Chk2 are specifically activated depending on the type of DNA damage and thus act in a complementary manner (Bartek and Lukas, 2003). Our results suggest that Chk1-dependent cell cycle arrest might serve as a backup system for DSBs that must be

repaired before completion of DNA replication or eliminated by Chk2-dependent apoptosis to prevent severe genomic instability and transformation of normal cells into cancer cells. In this regard, it should be noted that ATM regulates the recruitment of ATR to DSBs, leading to double-strand break-induced Chk1 phosphorylation (Adams *et al*, 2006; Jazayeri *et al*, 2006).

Surprisingly, neither Chk1 nor Chk2 was apparently involved in mouse senescence pathways, which may explain why tumour development in *Chk1*$^{+/-}$*Chk2*$^{+/-}$ and *Chk1*$^{+/-}$*Chk2*$^{-/-}$ mice had a late onset. These observations are in clear contrast with those observed in human cells, in which both Chk1 and Chk2 are activated after induction of premature or replicative senescence (d'Adda di Fagagna *et al*, 2003; Gire *et al*, 2004; Bartkova *et al*, 2006; Di Micco *et al*, 2006; Mallette *et al*, 2007). In addition, knockdown of Chk2 suppresses oncogene-induced senescence (Di Micco *et al*, 2006), and ectopic co-expression of dominant-negative forms of Chk1 and Chk2 (d'Adda di Fagagna *et al*, 2003) or Chk2 knockdown suppress replicative senescence in human cells (Gire *et al*, 2004). In this regard, mouse cells do not undergo replicative senescence, because they possess far longer telomeres than human cells. Therefore, Chk2 might have a specific function in the induction of replicative senescence that is not observable in mice. We found that complete loss of Chk1 led to a senescence-like permanent growth arrest in MEFs. Intriguingly, constitutive activation of ATR in mouse cells can also induce senescence (Toledo *et al*, 2008). We and others reported that Chk1 localizes at chromatin under unperturbed conditions and its phosphorylation by ATR releases Chk1 from chromatin (Smits *et al*, 2006; Niida *et al*, 2007). Chromatin-bound Chk1 is required for the expression of various cell cycle regulatory genes through phosphorylation of H3-T11 (Shimada *et al*, 2008). Therefore, constitutive activation of ATR mimics loss of Chk1 bound on chromatin. Taken together, these results indicate that permanent loss of Chk1 from chromatin can drive cells into senescence through epigenetic modifications on cell cycle gene promoters. This appears to be consistent with the apparently dispensable function of Chk1 in the induction of premature senescence.

In conclusion, our results suggest that a combination of partial defects in several tumour-protective barriers might engender a more progressive cancer-prone condition than a severe defect in one mechanism. This is in agreement with the association between genetic variations or mutations in *Chk1* and *Chk2* genes and the high cancer risk. Therefore, inhibition of Chk1 or Chk2 as an approach to cancer therapy should be undertaken with careful consideration.

Materials and methods

Immunoblotting

For preparation of whole cell extracts, cells were lysed in IP kinase buffer as previously described. The antibodies used for immunoblotting or immunofluorescence were directed against p53 (NCL-p53-505, Novocasta Laboratory), p21 (sc-6246, SantaCruz), p16 (sc-1207, SantaCruz), Cdc25A (sc-7389, SantaCruz), Che-1 (ab39631, Abcam), Mdm2 (sc-965, SantaCruz), Mdmx (sc-28222, SantaCruz), PAX5 (sc-1974, SantaCruz), CD3 (ab49943, Abcam), β-actin (ab2676-100, Abcam), phosphor-Ser-10-histone H3 (06-570, Upstate) and BrdU (B44, BD for IdU; BI1/75, ICR1 for CIdU).

Mice and MEFs

Chk1$^{+/-}$ mice (Takai *et al*, 2000) were crossed with *Chk2*$^{+/-}$ mice (Takai *et al*, 2002) to obtain *Chk1*$^{+/-}$*Chk2*$^{+/-}$ mice. Experimental cohorts were derived from littermates obtained from double-heterozygote breeders. All mice studied had a mixed 129 × C57BL/6 genetic background and were genotyped by PCR. All experiments were performed in compliance with the Nagoya City University Animal Care Committee guidelines. Primary MEFs were derived from E14.5 embryos of double-heterozygote breeders.

Cell cycle, apoptosis analysis and comet assay

The mitotic index was measured as described previously using anti-phosphor-Ser-10-histone H3 (06-570, Upstate) antibodies (Niida *et al*, 2005). For G1/S checkpoint analysis, primary MEFs were labelled with CIdU (10 μM) for 1 h, then treated with mock or IR (5 Gy) and additionally labelled with IdU (10 μM) for 1 h after incubation with fresh medium for 1 h (Figure 2A). The cells were then fixed in three parts methanol: one part glacial acetic acid at −20°C for 30 min, after which they were treated with 2 N HCl for 30 min. The cells were then washed with PBS, permeabilized with 0.05% Triton X-100 in PBS and blocked with 5% FBS, 0.2% Triton X-100 and 0.1% BSA in PBS. CldU was detected with a 1/100 dilution of anti-BrdU rat monoclonal antibody (BU1/75: ab6326, Abcam), and IdU was detected with a 1/50 dilution of anti-BrdU mouse antibody (clone B44: 347580, BD Biosciences). Clone B44 recognizes both IdU and CldU, but washing for 30 min with a high salt buffer (100 mM Tris, 0.5 M NaCl, 0.5% Tween, pH 8.0) releases it from CldU. A 1/500 dilution of Alexa 594-conjugated goat anti-rat IgG was used to detect BU1/75, and a 1/500 dilution of Alexa 488-conjugated goat anti-mouse IgG was used to detect B44. The cover slips were then mounted onto slides with Mowiol Mounting Medium for Fluorescence with 4′, 6′-diamidino-2-phenylindole (DAPI. For intra-S phase checkpoint analysis, primary MEFs were cultured with medium containing 10 nCi/ml [^{14}C] thymidine (Amersham) for 24 h, washed with PBS and cultured again for 30 min in medium without [^{14}C] thymidine. The cells were then X-irradiated (10 Gy), cultured for 1 h and then pulse labelled with medium containing 2.5 μCi/ml [^{3}H] thymidine for 30 min. The labelled cells were harvested and fixed in ice-cold 70% ethanol overnight. The fixed cells were applied to membranes on the filtration plate, and the membranes were washed with 70% ethanol and then 95% ethanol (Nalgen Nunc; no. 255984). Radioactivity on the membranes was determined with a liquid scintillation counter. Radio-resistant DNA synthesis was determined by the radioactivity of [^{3}H] divided by that of [^{14}C]. For apoptosis analysis, thymocytes were irradiated and cultured for 24 h. Cells were fixed, stained with propidium iodide and analysed by FACS. An alkaline-comet assay was performed using the OxiSelect™Comet Assay kit according to the manufacturer's instructions (CELL BIOLABS INC). DNA was stained with Vista Green DNA Dye.

Isolation of CD19-positive B cells

Splenocytes were obtained by dissection of *Chk1/Chk2* double-mutant mice and by manual disruption of the organ. The cell suspension was passed through a BD Falcon cell strainer (REF352340), and centrifuged at 300 *g* for 10 min at 4°C and suspended in 500 μl MACS running buffer. CD19-positive B cells were selected from single-cell suspensions of splenocytes by labelling the cells with magnetic bead-conjugated antibodies against CD19 (Miltenyi Biotec, 130-052-201), followed by Auto-MACS magnetic bead sorting according to the manufacturer's instructions. The CD19-positive cells (2×10^6) were stimulated by 25 μg/ml lipopolysaccharide for 72 h and treated with 0.1 ng/ml colcemid for an additional 2 h. The resultant cells were then subjected to karyotype analysis.

Retroviral-mediated gene transfer

To prepare retroviral particles, PlatE cells (2×10^6) were plated on a 10 cm culture dish, and then transfected with retroviral vectors using FuGene6 (Roche). For infection, primary MEFs at passage 2 were plated at a density of 2×10^5 cells per 10 cm dish and infected by virus from PlatE cells for 24 h. The infection process was repeated four times at 4–12 h intervals. After selection in the presence of 2 μg/ml puromycin for 4 days, growth curves, immunoblotting and senescence analysis of MEFs was carried out. To determine senescence, MEFs were stained for SA-β-gal activity as described previously (Bartkova *et al*, 2006; Di Micco *et al*, 2006). For retroviral transfection of E6 and E7 vectors, infected MEFs were selected in medium containing 100 μg/ml hygromycin for 4 days.

Supplementary data
Supplementary data are available at *The EMBO Journal* Online (http://www.embojournal.org).

Acknowledgements

We thank Drs Nakayama and Nishiyama for analysis of E7.5 embryos, Drs Hayashi and Sakai for anti-Cdc25A antibodies, Dr Yamada-Namikawa, Miss Morimoto, Miss Kojima, Mr Seeni_mohamed and Mr Tang for technical assistance. This work was supported in part by the Ministry of Education, Science, Sports and Culture of Japan through a Grant-in-Aid for Scientific Research on Priority Area (A), a grant for Scientific Research (B), the project for realization of regenerative medicine of MEXT and by the Mitsubishi Foundation, the Naito Memorial Foundation, the Toyoaki Foundation, the Takeda Foundation and the Uehara Foundation awarded to MN. The study was also partially supported by the Intramural Research Program of the NIH, National Cancer Institute.

Author contributions: HN and KM performed the majority of the experiments and data analysis. MS, KO, KO, KS, HF, AKK, BB, PMH, TM IM, TS, NM, MD and EA provided experimental data. HN, MD, NM and EA helped to write the paper. MN conceived of the project, planned and guided the research, and wrote the paper.

Conflict of interest

The authors declare that they have no conflict of interest.

References

Adams KE, Medhurst AL, Dart DA, Lakin ND (2006) Recruitment of ATR to sites of ionising radiation-induced DNA damage requires ATM and components of the MRN protein complex. *Oncogene* **25:** 3894–3904

Ahn J, Urist M, Prives C (2003) Questioning the role of checkpoint kinase 2 in the p53 DNA damage response. *J Biol Chem* **278:** 20480–20489

Antoni L, Sodha N, Collins I, Garrett MD (2007) CHK2 kinase: cancer susceptibility and cancer therapy—two sides of the same coin? *Nat Rev Cancer* **7:** 925–936

Appella E, Anderson CW (2001) Post-translational modifications and activation of p53 by genotoxic stresses. *Eur J Biochem* **268:** 2764–2772

Bartek J, Lukas J (2001) Pathways governing G1/S transition and their response to DNA damage. *FEBS Lett* **490:** 117–122

Bartek J, Lukas J (2003) Chk1 and Chk2 kinases in checkpoint control and cancer. *Cancer Cell* **3:** 421–429

Bartkova J, Horejsi Z, Koed K, Kramer A, Tort F, Zieger K, Guldberg P, Sehested M, Nesland JM, Lukas C, Orntoft T, Lukas J, Bartek J (2005) DNA damage response as a candidate anti-cancer barrier in early human tumorigenesis. *Nature* **434:** 864–870

Bartkova J, Rezaei N, Liontos M, Karakaidos P, Kletsas D, Issaeva N, Vassiliou LV, Kolettas E, Niforou K, Zoumpourlis VC, Takaoka M, Nakagawa H, Tort F, Fugger K, Johansson F, Sehested M, Andersen CL, Dyrskjot L, Ornтoft T, Lukas J *et al* (2006) Oncogene-induced senescence is part of the tumorigenesis barrier imposed by DNA damage checkpoints. *Nature* **444:** 633–637

Bell DW, Varley JM, Szydlo TE, Kang DH, Wahrer DC, Shannon KE, Lubratovich M, Verselis SJ, Isselbacher KJ, Fraumeni JF, Birch JM, Li FP, Garber JE, Haber DA (1999) Heterozygous germ line hCHK2 mutations in Li-Fraumeni syndrome. *Science* **286:** 2528–2531

Bertoni F, Codegoni AM, Furlan D, Tibiletti MG, Capella C, Broggini M (1999) CHK1 frameshift mutations in genetically unstable colorectal and endometrial cancers. *Genes Chromosomes Cancer* **26:** 176–180

Bruno T, De Nicola F, Iezzi S, Lecis D, D'Angelo C, Di Padova M, Corbi N, Dimiziani L, Zannini L, Jekimovs C, Scarsella M, Porrello A, Chersi A, Crescenzi M, Leonetti C, Khanna KK, Soddu S, Floridi A, Passananti C, Delia D *et al* (2006) Che-1 phosphorylation by ATM/ATR and Chk2 kinases activates p53 transcription and the G2/M checkpoint. *Cancer Cell* **10:** 473–486

Cao L, Kim S, Xiao C, Wang RH, Coumoul X, Wang X, Li WM, Xu XL, De Soto JA, Takai H, Mai S, Elledge SJ, Motoyama N, Deng CX (2006) ATM-Chk2-p53 activation prevents tumorigenesis at an expense of organ homeostasis upon Brca1 deficiency. *EMBO J* **25:** 2167–2177

Chehab NH, Malikzay A, Stavridi ES, Halazonetis TD (1999) Phosphorylation of Ser-20 mediates stabilization of human p53 in response to DNA damage. *Proc Natl Acad Sci USA* **96:** 13777–13782

Chellappan S, Kraus VB, Kroger B, Munger K, Howley PM, Phelps WC, Nevins JR (1992) Adenovirus E1A, simian virus 40 tumor antigen, and human papillomavirus E7 protein share the capacity to disrupt the interaction between transcription factor E2F and the retinoblastoma gene product. *Proc Natl Acad Sci USA* **89:** 4549–4553

Courtois-Cox S, Jones SL, Cichowski K (2008) Many roads lead to oncogene-induced senescence. *Oncogene* **27:** 2801–2809

Craig AL, Chrystal JA, Fraser JA, Sphyris N, Lin Y, Harrison BJ, Scott MT, Dornreiter I, Hupp TR (2007) The MDM2 ubiquitination signal in the DNA-binding domain of p53 forms a docking site for calcium calmodulin kinase superfamily members. *Mol Cell Biol* **27:** 3542–3555

d'Adda di Fagagna F, Reaper PM, Clay-Farrace L, Fiegler H, Carr P, Von Zglinicki T, Saretzki G, Carter NP, Jackson SP (2003) A DNA damage checkpoint response in telomere-initiated senescence. *Nature* **426:** 194–198

Di Micco R, Fumagalli M, Cicalese A, Piccinin S, Gasparini P, Luise C, Schurra C, Garre M, Nuciforo PG, Bensimon A, Maestro R, Pelicci PG, d'Adda di Fagagna F (2006) Oncogene-induced senescence is a DNA damage response triggered by DNA hyper-replication. *Nature* **444:** 638–642

Ghosh JC, Izumida Y, Suzuki K, Kodama S, Watanabe M (2000) Dose-dependent biphasic accumulation of TP53 protein in normal human embryo cells after X irradiation. *Radiat Res* **153:** 305–311

Gire V, Roux P, Wynford-Thomas D, Brondello JM, Dulic V (2004) DNA damage checkpoint kinase Chk2 triggers replicative senescence. *EMBO J* **23:** 2554–2563

Gorgoulis VG, Vassiliou LV, Karakaidos P, Zacharatos P, Kotsinas A, Liloglou T, Venere M, Ditullio Jr RA, Kastrinakis NG, Levy B, Kletsas D, Yoneta A, Herlyn M, Kittas C, Halazonetis TD (2005) Activation of the DNA damage checkpoint and genomic instability in human precancerous lesions. *Nature* **434:** 907–913

Hirao A, Cheung A, Duncan G, Girard PM, Elia AJ, Wakeham A, Okada H, Sarkissian T, Wong JA, Sakai T, De Stanchina E, Bristow RG, Suda T, Lowe SW, Jeggo PA, Elledge SJ, Mak TW (2002) Chk2 is a tumor suppressor that regulates apoptosis in both an ataxia telangiectasia mutated (ATM)-dependent and an ATM-independent manner. *Mol Cell Biol* **22:** 6521–6532

Hirao A, Kong YY, Matsuoka S, Wakeham A, Ruland J, Yoshida H, Liu D, Elledge SJ, Mak TW (2000) DNA damage-induced activation of p53 by the checkpoint kinase Chk2. *Science* **287:** 1824–1827

Jallepalli PV, Lengauer C, Vogelstein B, Bunz F (2003) The Chk2 tumor suppressor is not required for p53 responses in human cancer cells. *J Biol Chem* **278:** 20475–20479

Jazayeri A, Falck J, Lukas C, Bartek J, Smith GC, Lukas J, Jackson SP (2006) ATM- and cell cycle-dependent regulation of ATR in response to DNA double-strand breaks. *Nat Cell Biol* **8:** 37–45

Jin J, Ang XL, Ye X, Livingstone M, Harper JW (2008) Differential roles for checkpoint kinases in DNA damage-dependent degradation of the Cdc25A protein phosphatase. *J Biol Chem* **283:** 19322–19328

Kaneko YS, Watanabe N, Morisaki H, Akita H, Fujimoto A, Tominaga K, Terasawa M, Tachibana A, Ikeda K, Nakanishi M (1999) Cell-cycle-dependent and ATM-independent expression of human Chk1 kinase. *Oncogene* **18:** 3673–3681

Lam MH, Liu Q, Elledge SJ, Rosen JM (2004) Chk1 is haploinsufficient for multiple functions critical to tumor suppression. *Cancer Cell* **6:** 45–59

Lee JS, Collins KM, Brown AL, Lee CH, Chung JH (2000) hCds1-mediated phosphorylation of BRCA1 regulates the DNA damage response. *Nature* **404:** 201–204

Liu Q, Guntuku S, Cui XS, Matsuoka S, Cortez D, Tamai K, Luo G, Carattini-Rivera S, DeMayo F, Bradley A, Donehower LA, Elledge SJ (2000) Chk1 is an essential kinase that is regulated by Atr and